



# Optimizing microgrid design and operation: A decision-making framework for residential distributed energy systems in Brazil

Ana Paula Alves Amorim<sup>a</sup>, Karen Valverde Pontes<sup>a</sup>, Bogdan Dorneanu<sup>b</sup>, Harvey Arellano-Garcia<sup>b,\*</sup>

<sup>a</sup> Industrial Engineering Program, Federal University of Bahia, Salvador da Bahia, Brazil

<sup>b</sup> FG Prozess, und Anlagentechnik, Brandenburgische Technische Universität Cottbus-Senftenberg, Cottbus, Germany

## ARTICLE INFO

**Keywords:**  
 Distributed energy systems (DES)  
 Microgrid optimization  
 Mixed-integer nonlinear programming (MINLP)  
 Renewable energy incentives  
 Time-dependent efficiency

## ABSTRACT

This paper explores the optimization of microgrid design and operation for residential distributed energy systems in Brazil, addressing the growing demand for sustainable energy in the context of climate change. A decision-making framework based on Mixed-Integer Nonlinear Programming (MINLP) is proposed to integrate distributed energy resources (DERs) such as solar, wind, and biogas. Key challenges include managing the variability of renewable resources and complying with local regulations, while also addressing gaps in literature, particularly the impact of time-dependent efficiency profiles on energy sharing within microgrids. By employing innovative analyses and clustering techniques, the research optimizes microgrid configurations, accounting for seasonal demand fluctuations and the influence of incentive policies on system feasibility. The findings reveal that incorporating a time-dependent efficiency model can reduce total costs by 45 %. This reduction underscores the importance of accurate efficiency predictions, as the model captures variations in energy generation and utilization efficiency over time, improving system optimization. Additionally, the findings reveal that a well-structured optimization model can meet 100 % of electricity and hot water demands across all scenarios, with customized incentives playing a crucial role in reducing costs and promoting sustainability.

## 1. Introduction

Global warming has increased incentives for renewable sources, creating favorable conditions for investment in distributed generation systems. Microgrids, which combine local generation with intelligent energy management, provide an alternative to centralized power systems by integrating different Distributed Energy Resources (DERs) and loads. These systems help reduce greenhouse gas emissions, diversify the energy matrix, minimize transmission losses, and create jobs (Lee et al., 2015). A key factor in the success of microgrids is the integration of energy networks – i.e., electricity, heating, hot water, and cooling – across residential, commercial, and industrial sectors, maximizing synergies among them (Zatti et al., 2019).

Microgrid planning is complex task due to the need to manage the variability of renewable energy sources like solar and wind, which fluctuate based on time and weather conditions. This requires accurate forecasting and real-time monitoring to maintain energy availability. Mixed-Integer Linear Programming (MILP) models have been applied to

optimize the design and operation of microgrids, dealing with the challenge of integrating multiple energy sources and meeting diverse energy demands (Ren et al., 2022). Geographic location and local regulations further complicate planning, as they affect resource availability and operating conditions (Gamara and Guerrero, 2015). Improper allocation of renewable resources can lead to inefficiencies, protection system reconfigurations, and increased costs (Tan et al., 2013). A detailed analysis is needed to determine the optimal configuration of a microgrid before implementing.

Recent literature has also addressed the impact of COVID-19 pandemic on energy consumption patterns. The pandemic has caused significant shifts in energy demand due to increased remote working and changes in residential energy usage. Studies have shown that residential energy consumption patterns have altered dramatically, with increase in electricity use for home offices and reduction in commercial energy use (Chinthavali et al., 2022). This shift has implications for microgrid design, particularly in adjusting to new demand profiles and optimizing energy management strategies under pandemic conditions. The incorporation of COVID-19 scenarios into microgrid optimization models is

\* Corresponding author.

E-mail address: [arellano@b-tu.de](mailto:arellano@b-tu.de) (H. Arellano-Garcia).

<b>Nomenclature</b>	
<i>Continuous variables and abbreviations</i>	
$A_i^{tech}$	Area of each technology $tech \in \{PV, SC, WT\}$ in house $i$ ( $m^2$ )
$ACCOP$	Air conditioning power coefficient
$C_{BUY}^{GRID}$	Total cost of electricity purchased from the grid (R\$)
$C_{ENV}$	Total environmental costs (R\$)
$C_{Fix}^{NG}$	Fixed monthly cost of purchasing natural gas (R\$/month)
$C_{INV}$	Total investment (R\$)
$C^{NG}$	Cost of natural gas purchased from the grid (R\$)
$C_{OM}$	Operating and maintenance cost (R\$)
$CI^{tech}$	Carbon intensity of each technology $tech$ (kg CO <sub>2</sub> /kWh)
$C_{TOTAL}$	Total annual investment and annual operation cost (R\$)
$c_p^{water}$	heat capacity of water and corresponds to (kJ/kg)
$Cp^{WT}$	Power coefficient of the wind turbine
$CRF$	Capital recovery rate
$CT$	Carbon tax (R\$/ kg CO <sub>2</sub> )
$d_m$	Number of days in season $m$
$DMO$	Density of the dry material in the fluid (kg/m <sup>3</sup> )
$E_j$	Numerical position of house $j$
$E_{i,m,p}^{tech}$	Thermal energy produced by $tech \in \{BH, GH, SC, BG\}$ in house $i$ in time period $(m, p)$ (kW)
$E_{i,m,p}^{AC}$	Cooling air produced in house $i$ in each period $(m, p)$ (kW)
$E_{i,m,p}^{ES}$	Thermal energy produced for the electric shower in house $i$ in time period $(m, p)$ (kW)
$E_{i,m,p}^{GRID}$	Amount of power purchased from the central grid (kW)
$E_{i,m,p}^{SALE}$	Amount of energy inserted into the central grid by house $i$ in period $m, p$ (kW)
$E_{i,m,p}^{SALE,tech}$	Amount of energy produced by technology $tech$ inserted into the central grid by house $i$ in period $m, p$ (kW)
$E_{i,m,p}^{SELF}$	Amount of energy generated for self-consumption by house $i$ in period $m, p$ (kW)
$E_{i,m,p}^{STORAGE}$	Amount of stored energy in house $i$ in period $m, p$ (kW)
$E_{i,m,p}^{STORAGE,BT}$	Amount of electricity in the storage unit at any time (kW)
$E_{i,m,p}^{STORAGE IN,BT}$	Energy loaded into the battery (kW)
$E_{i,m,p}^{STORAGE OUT,BT}$	Energy removed from the battery (kW)
$E_{i,j,m,p}^{TRANSFER}$	Amount of energy transferred from house $i$ to house $j$ in period $m, p$ (kW)
$E_{i,j,m,p}^{TRANSFER,res}$	Amount of resource (res: HW, E) transferred from house $i$ to house $j$ in period $m, p$ (kW)
$E_{i,m,p}^{GRID,r}$	Amount of energy purchased from the central grid house $i$ in period $m, p$ (kW)
$E_{i,m,p}^{SELF,tech,r}$	Amount of resource (r: HW, E) produced by technology $tech$ for self-use in house $i$ in period $m, p$ (kW)
$E_{i,m,p}^{STORAGE OUT,tech,r}$	Energy removed from the storage technology $tech$
$E_{j,i,m,p}^{TRANSFER,r}$	Energy (r: HW, hot water; E, electricity) transferred from house $i$ to house $j$ at any time $(m, p)$
$FIT$	Revenue received for adopting Feed in Tariff (R\$)
$G_{i,m,p}^{NG}$	Natural gas used for cooking (kW)
$h_p$	Total of hours within time period $p$
$Hb$	Calorific capacity of biogas (kWh/m <sup>3</sup> )
$HW_{i,m,p}^{STORAGE,SC}$	Hot water produced by solar collector in house $i$ at any time any time $(m, p)$ and stored (L/h)
$HW_{i,m,p}^{TS}$	Hold up of hot water in the tank (L) at any time $(m, p)$
$HW_{i,m,p}^{TS,in}$	Hot water inserted into thermal storage at any time $(m, p)$
$HW_{i,m,p}^{TS,out}$	Mass of hot water that leaves the tank at any time $(m, p)$
$HW_{i,m,p}^{tech}$	Amount of hot water produced by $tech \in \{BH, ES, GH, SC\}$ in house $i$ at any time period $(m, p)$ (L)
$HW_{i,j,m,p}^{TRANSFER}$	Amount of hot water transferred from house $i$ to house $j$ (L)
$IS$	Percentage of dry mass in organic material
$It_{m,p}$	Solar irradiation (kWh/m <sup>2</sup> )
$k_i^{tech}$	Power of $tech \in \{AC, BG, BT, ES, GH\}$ in house $i$ (kW)
$k_i^{TS}$	Storage tank capacity in house $i$ (L)
$K_0, K_1$	Koehl correlation coefficient
$KL$	Coefficient of power loses in diodes
$Load_{i,m,p}^r$	Energy demand for each resource $r$ , as electricity (E), hot water (HW), air conditioning (AC), and cooking gas (C) in house $i$ at period $m, p$ (kW)
$n$	Component lifetime (years)
$ne^{tech}$	Efficiency of $tech \in \{BG, ES, GH\}$
$nee^{PV}$	Nominal energy efficiency of the photovoltaic panel
$ne_{i,m,p}^{PV}$	Time-varying energy efficiency of the photovoltaic panel
$ne_{i,m,p}^{SC}$	Time-varying energy efficiency of the solar collector
$NEM$	Credit revenue obtained by using the Net Metering policy
$O_i$	Numerical position of house $j$
$P^{FIT,tech}$	Rate of the sale for the technology $tech$ (R\$/kW)
$P^{NG}$	Price of gas (R\$/m3)
$PV_{up}$	Upper limit for installing PV panels and solar collectors
$P_{m,p}^{elec}$	Price of electricity for each period of time $m, p$ (R\$/kWh)
$q^{NG}$	Calorific capacity of natural gas (kWh/m <sup>3</sup> )
$Qbg$	Volume of biogas produced (m <sup>3</sup> )
$Qbgh_{i,m,p}$	Biogas production for hot water for house $i$ in time period $(m, p)$ (m <sup>3</sup> )
$Qbgc_{i,m,p}$	Biogas production for cooking food for house $i$ in time period $(m, p)$ (m <sup>3</sup> )
$Qbgg_{i,m,p}$	Biogas production for electricity generation for house $i$ in time period $(m, p)$ (m <sup>3</sup> )
$Qbio_{i,m,p}$	Total biogas production by house $i$ in time period $(m, p)$ (m <sup>3</sup> )
$Qom_i$	Organic matter produced in each house per day (kg)
$Qow_i$	Amount of organic material purchased from house $i$ (kg)
$r$	Interest rate (%)
$s_m$	Number of months in each season $m$
$Sale_{up}$	Upper bound of energy that can be sold to the grid (kW)
$T_{m,p}^{Env}$	Ambient air temperature (°C)
$T_{i,m,p}^{PV/SC}$	Operating temperature of photovoltaic panel and solar collector (°C)
$T_{storage}$	Desired temperature of hot water (°C)
$tr$	Hydraulic retention time in the biodigester (day)
$Use_{i,m,p}^{NG}$	Amount of natural gas purchased from the grid by house $i$ in period $m, p$ (kW)
$V^{BD}$	Volume of the biodigestor (m <sup>3</sup> )
$V_{ci}$	Cut in speed (m/s)
$V_{co}$	Cut off speed of the turbine (m/s)
$V_{m,p}^{Env}$	Wind speed (m/s)
$V_r$	Nominal speed (m/s)
$X$	Battery load rate (%)
$WT_{up}$	Upper bound on wind turbine area
<i>Binary variables</i>	
$Y^{FIT}$	Use of the FIT policy
$Y^{NEM}$	Use of the NEM policy
$Y_{ij}^{MG}$	Existence of an electricity line between houses $i$ and $j$
$Y_{i,j}^P$	Existence of pipeline from house $i$ to house $j$

$Y_{i,m,p}^{GRID}$	Purchase of energy from the central grid by house $i$ and periods $m$ and $p$	$\beta_S$	Temperature coefficient for silicon photovoltaic panel
$Y_i^{NG}$	Use of natural gas	$\beta_{ij}$	Heat and electric loss
$Y_i^{SC}$	Production of energy in house $i$ by solar collector	$\theta$	Battery static loss coefficient (%)
$Y_i^{WT}$	Existence of wind turbine in the house $i$	$\Delta X$	Battery discharge rate (%)
$Z$	Existence of the microgrid	$\zeta$	Loss coefficient for thermal storage
		$\rho_{water}$	Water density ( $\text{kg}/\text{m}^3$ )
		$\rho_{wind}$	Wind density ( $\text{kg}/\text{m}^3$ )

still emerging, with few studies addressing how pandemic-induced changes in energy consumption should be factored into system design and operation.

Despite the progress in microgrid research, there are gaps in the literature that need to be addressed. Table 1 provides a review of studies from the last 15 years on microgrid design, specifically those that focus on meeting multiple residential energy demands, such as electricity, heating, hot water, cooling, and cooking.

While many works focus on electricity and heating, few consider the full range of residential energy needs. Notably, Weber and Shah (2011) are among the few to examine hot water generation through solar collectors. Other researchers have used gas or biomass boilers to meet heating demands, highlighting alternative technologies, including pipeline (Clarke et al., 2021), microgrids (Sidnell et al., 2021a), or combinations (Sidnell et al., 2021b). The growing use of solar thermal energy in Brazil, which has reduced residential electricity consumption by 44 %, underscores the need to further explore its potential for hot water production (Weiss and Spörk-Dür, 2020).

Recently, due to its impact on the design and operation of the residential networks (Panda et al., 2023), variability in demand and availability of renewable resources has been included into the optimization superstructures. Advanced statistical models and machine learning techniques are usually implemented for short- and long-term demand forecasting (Fose et al. 2024), and the information utilized in scenario-based optimization (De Mel et al. 2023) that implement probabilistic (Li et al., 2023a) and stochastic models accounting for the uncertainties. Other developments focused on data-driven robust scheduling models (Li et al., 2023b).

Biogas remains an underutilized resource in microgrid design, despite its potential to generate both electricity and thermal energy with low environmental impact. As Table 1 indicates, few studies have explored the combined use of biogas, solar photovoltaics, wind energy, and solar thermal energy in microgrids, even though biogas offers a renewable alternative to natural gas. Most research on biogas has focused on rural electrification, while its potential to meet hot water and cooking gas demands in urban microgrids remains largely unexplored (Tooryan et al., 2020; Kamal et al., 2023).

Another gap in literature involves the time-dependent efficiency profiles of renewable resources and their impact on energy-sharing behavior in microgrids. The efficiency of renewable technologies like photovoltaic panels, solar collectors, and wind turbines varies with time and weather, affecting the real-time performance of microgrids. However, there has been little systematic analysis of how the determination of time periods for optimization affects the allocation and sizing of renewable resources, particularly in residential systems.

Incentive policies have played a critical role in encouraging the adoption of distributed renewable energy systems worldwide (Freitas et al., 2015). However, these policies must be tailored to the specific conditions of each region to be effective. Despite their importance, incentive policies such as Feed-in-Tariffs and Renewable Heat Incentives are often overlooked in microgrid optimization models. For instance, although the UK offered the Feed-in-Tariff policy, studies like Weber and Shah (2011) and Zhang et al. (2015) did not account for this when assessing microgrid feasibility. Conversely, other studies concluded that such policies enhance the feasibility of distributed energy generation

### Greek letters

$\beta_S$	Temperature coefficient for silicon photovoltaic panel
$\beta_{ij}$	Heat and electric loss
$\theta$	Battery static loss coefficient (%)
$\Delta X$	Battery discharge rate (%)
$\zeta$	Loss coefficient for thermal storage
$\rho_{water}$	Water density ( $\text{kg}/\text{m}^3$ )
$\rho_{wind}$	Wind density ( $\text{kg}/\text{m}^3$ )

systems (Clarke et al., 2021; Sidnell et al., 2021a, 2021b). Omu et al. (2013) demonstrated that the decision to implement renewable energy subsidies is highly dependent on regulatory frameworks and building requirements.

To address these research gaps, this paper proposes an optimization framework for the design and operation of residential microgrids. The models use Mixed-Integer Nonlinear Programming (MINLP) to explore the optimal integration of renewable energy sources, time-dependent efficiency profiles, and incentive policies. Additionally, it examines the impact of COVID-19 on energy consumption patterns, incorporating various pandemic scenarios into the optimization framework.

The novel aspects of this study can be delineated as follows:

- Time-dependent efficiency profiles.* While several recent studies have discussed renewable resource variability, this contribution integrates a clustering-based method to discretize time-dependent efficiencies.
- Comprehensive energy needs.* Unlike most recent works that focus solely on electricity or heating, the current study addresses a broader range of residential energy demands, including electricity, hot water, cooling, and cooking gas, offering a more holistic approach to microgrid optimization.
- Integration of pandemic scenarios.* The optimization framework incorporates various COVID-19 scenarios to assess the pandemic's impact on energy consumption patterns, an aspect not extensively addressed in recent literature.
- Brazil-specific scenarios.* This contribution uniquely considers the regulatory and environmental context of Brazil, including the potential of underutilized resources like biogas and the impact of solar thermal adoption, which has distinct implications for microgrid design in tropical and subtropical regions.

Although the study is presented in a Brazil-specific context, the optimization framework is designed to be adaptable and easily applicable to other regions. By incorporating generalized approaches to time-dependent efficiencies, energy-sharing strategies, or incentive policies, the framework provides a versatile tool for diverse regulatory, climatic, and resource conditions.

The paper is structured as follows: the next section describes the renewable resources considered, the methodology for splitting the time horizon, and the optimization problem formulation. The results section presents the optimal solutions for various scenarios, emphasizing the importance of clustering for time-horizon discretization and time-dependent efficiencies. The paper concludes with a discussion of the main findings and contributions.

## 2. Problem definition

This study develops an optimization model for residential microgrids using Brazil as a case study. The Brazilian electricity matrix is notable for its high proportion of renewable energy sources, comprising 86 % of the total (46 % hydropower, 20 % solar, 13 % wind, and 7 % biomass) (Absolar, 2024). In 2023, Brazil was ranked 8th globally for installed PV capacity, with a capacity addition of 24 GW (Global Solar Council, 2024). Of the 47 GW of installed PV capacity in 2024, 15 GW are from centralized generation and 32 GW from distributed generation (Absolar,

**Table 1**  
Recent studies on microgrid configuration optimization.

Demand	Energy/ heat sources	Incentive policy	Site	Reference
Electricity, heating	PV, WT, CHP	-	UK	Hawkes, Leach (2009)
Electricity, heating, hot water, air cooling	PV, WT, CHP, GB, SC	-	UK	Weber and Shah (2011)
Electricity, heating	PV, GB, CHP	FIT	Greece	Mehler et al. (2012)
Electricity, heating	PV, WT, BB, GB	FIT, RHI	UK	Omu et al. (2013)
Electricity, heating, hot water, air cooling	GB, EH, CHP	-	Japan	Wakui, Yokoyama (2014)
Electricity, heating	PV, WT, CHP, Abs	FIT	Australia	Wouters et al. (2015)
Electricity, heating	CHP	FIT	UK	Zhang et al. (2015)
Electricity, gas for cooking	PV, BT, BG	-	Kenya	Nasir and Mutale (2016)
Electricity, heating	PV, SC, BT	-	Switzerland	Gabrielli et al. (2018)
Electricity, heating, hot water, air cooling	PV, CHP, BT, GB, EC	-	Alasca	Mashayekh et al. (2018)
Electricity, heating	PV, CHP, GB, BT	FIT	Germany	Schütz et al. (2018)
Electricity, heating	PV, CHP, BB, GB, BT	FIT	Switzerland	Mavromatidis et al. (2018)
Electricity, heating, cooling	PV, SC, GB, ICE, TS	-	Italy	Zatti et al. (2019)
Electricity, heating	PV, CHP, GB	FIT	UK	De Mel et al. (2020)
Electricity, heating	PV, EH, BT	-	Germany	Teichgraeber et al. (2020)
Electricity, heating, cooling	PV, WT, BT, GB, BB, TS	-	Hawaii	Tooryan et al. (2020)
Electricity, heating, hot water, air cooling	PV, WT, CHP, BT, BB, GB, GH, Abs, AC, TS	FIT	UK	Clarke et al. (2021)
Electricity, heating, hot water, air cooling	PV, WT, CHP, BT, BB, GB, GH, Abs, AC, TS	FIT, RHI	UK	Sidnell et al. (2021a)
Electricity, heating, hot water, air cooling	PV, WT, CHP, BT, BB, GB, GH, Abs, AC, TS	FIT, RHI	UK	Sidnell et al. (2021b)
Electricity, heating	PV, CHP	-	Greece	Mehler et al. (2022)
Electricity, heating	PV, WT, ES, EB	FIT	China	Li et al. (2023b)
Electricity	PV	-	Australia	Shi et al. (2023)
Electricity, heating	PV, CHP, GB	FIT	UK	De Mel et al. (2023)
Electricity	PV, WT, ES, EV, FC	FIT	NA	Seyedeh-Baragh et al. (2024)

PV: Photovoltaic; WT: Wind Turbine; GWP: Global Warming Potential of the components; RHI: Renewable Heat Incentive; Abs: Absorption Chillers; EC: Electric Chiller; EH: Electric Water Heater; BB: Biomass boiler; GB: Gas boiler; EB: Electric boiler; GH: Gas heater; ES: Electricity storage; EV: Electric vehicle; FC: Fuel cell; TS: Thermal Storage; SC: Solar Collector; CHP: Combined Heat and Power.

2024). Despite the exponential growth in the last 4 years, distributed PV energy serves only 13 % of Brazil's 91 million electricity consumers, highlighting significant growth potential (Absolar, 2024; Abgd, 2024).

Brazil is ranked 6th globally for wind energy installed capacity since 2021, with wind power contributing 32 MW in 2024, representing less than 1 % of the country's distributed energy (Agência Brasil, 2023; Absolar, 2024). The low percentage is partly due to the uneven distribution of wind resources and the high costs associated with larger wind turbines, as well as the limited adoption of residential wind turbines. In 2023, global installed biomass energy capacity was approximately 150 GW, with Brazil accounting for 17 GW (Statista, 2024; Absolar, 2024). However, despite the 2012 Normative Resolution regulating distributed micro and mini generation, such systems still represented less than 7 % of Brazil's total installed capacity in 2024 (Absolar, 2024).

The proposed framework addresses the energy demands for electricity, hot water, cooking gas, and cooling air in residential settings. It aims to determine the optimal combination and sizing of distributed renewable sources for a set of houses. Although Fig. 1 illustrates a model with three houses, it can be scaled up to accommodate more.

Electricity needs can be met by wind, photovoltaic, or biogas resources, or by purchasing from the central grid. Renewable electricity can be used for self-consumption, transferred to other households, fed into the central grid, or stored in batteries. For hot water, options include electric showers, biogas heaters, solar collectors, or gas heaters. Thermal storage is considered to leverage solar energy variations, and hot water sharing among households is facilitated. It is crucial to ensure that electric showers do not operate simultaneously with other hot water technologies to avoid conflicts.

Cooking gas can be supplied either by natural gas from the network or by biogas produced in a biodigester. The biodigester is centrally located to manage space limitations and avoid unpleasant odors in residential areas. It collects organic waste from all connected houses and allows for biogas transportation based on each household's demand. Additionally, there is an option to purchase extra organic material for the biodigester.

Several assumptions are considered to simplify the models and reduce their computational load. Firstly, the proposed framework does not explicitly consider detailed factors such as wind turbulence, shading effects on solar panels, or humidity variations that could impact renewable energy generation. Furthermore, for the different energy generation and consumption technologies, the models consider only their capacity and efficiency. While the factors can influence the performance of the renewable systems, they lead to detailed simulations that are computationally expensive. Nonetheless, the impact of these factors on the results of the optimization is likely to be moderate, as the focus is on broader trends rather than highly granular predictions. It is also important to note that efficiency of the different technologies is not assumed to be constant, but modelled to reflect more realistic, although simplified, variations based on the operational conditions of the technologies considered.

Regarding the representation of the microgrid and pipeline networks, the framework assumes a simplified representation of the hot water pipeline treating it as a basic flow system without accounting for detailed physical behavior such as pressure drop or fluid dynamics (Clarke et al., 2021). Heat and electricity losses are included and considered to depend linearly on the length of the cable or pipe, respectively. This simplification was made to reduce model complexity and computational burden.

## 2.1. Splitting the time horizon

The microgrid operates on an annual time horizon, divided into representative seasons – spring, summer, autumn, and winter – to balance model complexity and represent consumption profiles effectively while maintaining computational feasibility. To facilitate optimization and reduce computational effort, continuous time scales (day, month, year) are discretized into time periods. Brazil's climate exhibits distinct seasonal patterns, particularly in terms of resource availability (e.g., solar irradiance, wind speed, and biogas feedstock) and energy demand.

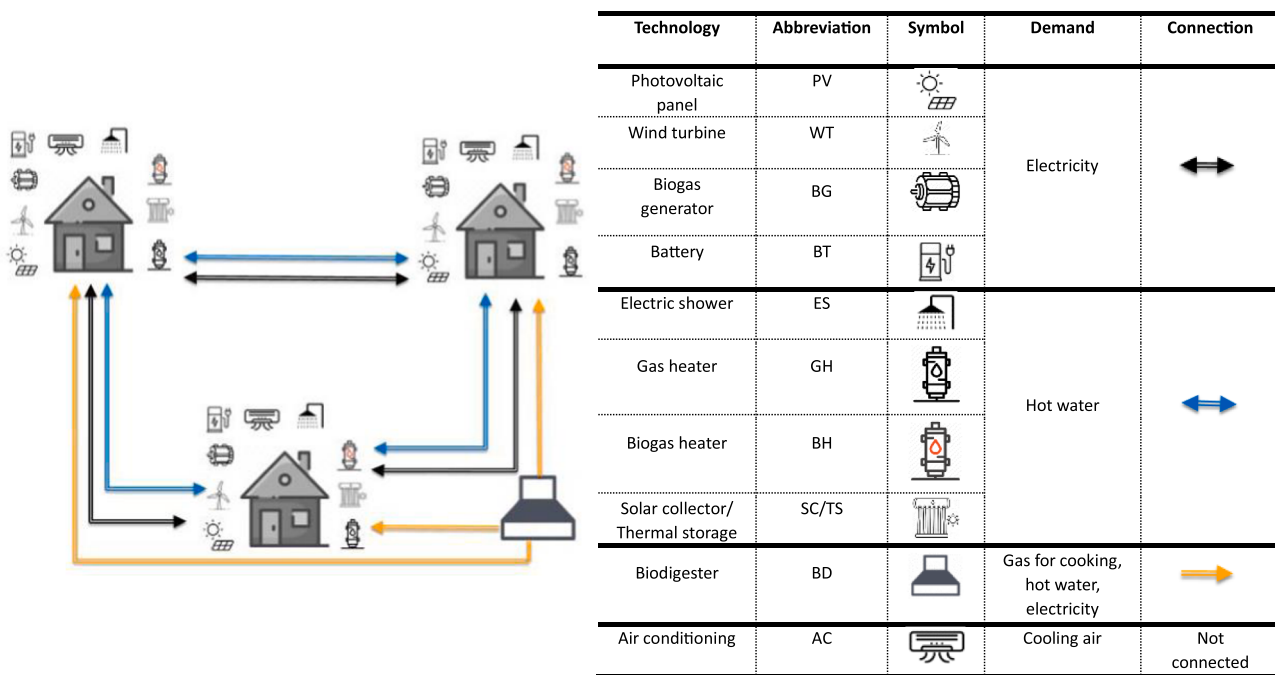


**Fig. 1.** Overview of microgrid technologies. Hot water sharing is shown with the blue line, electricity sharing with the black line, and biogas transfer with the yellow line.

A clustering method is used to capture these patterns rigorously to segment time periods based on demand profiles and environmental data (Zatti et al., 2019), which accurately reflect the most critical variations in resources and demand. This method enhances the robustness of the seasonal segmentation while keeping the problem size manageable. Such clustering-based segmentation is aligned with common practices in DER modelling, more empirical, which rely on manual observation and division as seen in Clarke et al. (2021) and Sidnell et al. (2021a). The clustering approaches address limitations of empirical method by identifying patterns and grouping similar data points into clusters.

The decision to simplify the annual horizon into representative seasons also addresses computational challenges inherent in solving the associated Mixed-Integer Nonlinear Programming (MINLP) problem. MINLP formulations for microgrid optimization involve nonconvex constraints, such as time-dependent efficiency profiles and nonlinear power balance equations. Using a global optimization solver, such as BARON, adds computational intensity due to its exhaustive search for globally optimal solutions. By employing clustering-based representative periods, the number of decision variables and constraints is reduced, mitigating computational load while maintaining the essential characteristics of the system's temporal behavior. This clustering-based simplification allows the model to balance temporal resolution and computational feasibility, ensuring tractability without sacrificing accuracy.

The K-means clustering technique (Yse, 2019) is central to this approach. In this method, each cluster is represented by a centroid, the arithmetic mean of its data points. The data series are first normalized to ensure consistency across different dimensions and units (e.g., electricity demand, environmental data, and prices). The clustering follows a two-step algorithm: initially, data are segmented into monthly clusters based on electricity demand, solar radiation, and wind speed. In the second step, these monthly clusters are further divided into hourly clusters, considering variations in hourly energy tariffs. The optimal number of clusters is determined using the elbow method (Patel et al., 2022), ensuring that the time periods are consecutive (e.g., 00:00–12:00, 12:00–18:00, and 18:00–00:00), and defining the number of months in each season  $m$  ( $s_m$ ), days in season  $m$  ( $d_m$ ), and total hours in each time period  $p$  ( $h_p$ ).

Addressing the challenges of variability and intermittency in renewable energy generation and demand is integral to the proposed framework. Instead of relying on a single condition for renewable resources, variability is captured through clustering methods, which identify representative periods derived from historical data. These periods reflect key patterns and fluctuations over the year, ensuring the design accounts for diverse conditions, including peak, average, and low-resource scenarios. The design thus balances computational tractability with practical accuracy, reducing risks of underperformance or overdesign. Clustering methods like K-means, incorporating centering and the elbow method, determine the optimal number of representative periods, capturing variability without introducing unnecessary complexity.

The K-means algorithm was implemented in Python using the *pandas*, *numpy* and *matplotlib* libraries (Rossum and Drake Jr., 1995). *Pandas* was used for data manipulation and analysis, *numpy* supported multi-dimensional array processing, and *matplotlib* facilitated data visualization and graph generation.

## 2.2. Optimization problem formulation

This section introduces the formulation of the optimization problem, with the objective function, followed by the design, capacity and demand constraints for electricity, cooling air, hot water, and cooking gas. Next, the operational, design, and capacity constraints for each technology are outlined. The indices  $i = 1, \dots, n$  or  $j = 1, \dots, n$  represent houses,  $m = 1, \dots, k$  denotes the season (defined by months), and  $p = 1, \dots, h$  refers to the time period (in hours). A complete list of variables is provided in the nomenclature for brevity.

### 2.2.1. Objective function

The optimization aims to minimize the total annual cost, which includes investment, operation, environmental costs, and energy transactions with the grid (Sidnell et al., 2021a):

$$C_{TOTAL} = C_{INV} + C_{OM} + C^{ENV} + C_{BUY}^{GRID} + C^{NG} - NEM - FIT \quad (1)$$

Here,  $C_{INV}$  represents the capital investment for each technology,

while  $C_{OM}$  includes the fixed and variable operational and maintenance costs, both detailed in the [Supplementary Material](#).

The annual investment cost,  $C_{INV}$  is calculated by summing up the capital cost of the different components of the network multiplied by a capital recovery factor (CRF) expressed as ([Clarke et al., 2021](#)):

$$CRF = \frac{r(1+r)^n}{(1+r)^n - 1} \quad (2)$$

where  $r$  is the interest rate (%), and  $n$  is the lifetime of the component (years).

The environmental cost  $C^{ENV}$  is based on each country's GHG reduction responsibilities, calculated as ([Sidnell et al., 2021a](#)):

$$\begin{aligned} C^{ENV} = CT \cdot & \left( \sum_{tech} \left( CI^{tech} \cdot \sum_{i,m,p}^{tech} E_{i,m,p}^{tech} \cdot d_m \cdot h_p \cdot s_m \right) + CI^{NG} \right. \\ & \left. \cdot \left( \sum_{i,m,p} Use_{i,m,p}^{NG} \cdot d_m \cdot h_p \cdot s_m \right) + CI^{BG} \cdot Qbg \cdot Hb \right) \end{aligned} \quad (3)$$

For  $tech \in \{GRID, PV, WT, SC\}$ .

The cost of buying electricity from the grid is:

$$C_{BUY}^{GRID} = \sum_{i,m,p} \left( E_{i,m,p}^{GRID} \cdot P_{m,p}^{Elec} \cdot d_m \cdot h_p \cdot s_m \right) \quad (4)$$

The cost of purchasing natural gas is:

$$C^{NG} = \frac{P^{NG}}{q^{NG}} \cdot \sum_{i,m,p} \left( Use_{i,m,p}^{NG} \cdot d_m \cdot h_p \cdot s_m \right) + \sum_i Y_i^{NG} \cdot C_{Fix}^{NG} \cdot s_m \quad (5)$$

where  $C_{Fix}^{NG}$  (R\$/month) is the fixed monthly cost of purchasing natural gas, and  $Y_i^{NG}$  is a binary variable indicating whether natural gas is used.

To evaluate the best incentive policy, two models are considered: Net Metering (NEM) and Feed in Tariff (FIT). The energy credits earned from NEM are:

$$NEM = \sum_{i,m,p} \left( E_{i,m,p}^{SALE,tech} \cdot P_{m,p}^{Elec} \right) \cdot d_m \cdot h_p \cdot s_m \cdot Y^{NEM} \quad (6)$$

For  $tech \in \{PV, WT, BG\}$ .

The revenue from FIT is ([Mehler et al., 2012](#)):

$$FIT = \sum_{i,m,p} \left( E_{i,m,p}^{SALE,tech} \cdot P_{m,p}^{FIT,tech} \right) \cdot d_m \cdot h_p \cdot s_m \cdot Y^{FIT} \quad (7)$$

$$E_{i,m,p}^{WT} = \begin{cases} 0, & \forall V_{co} < V_{m,p}^{Env} \cup 0 < V_{m,p}^{Env} < V_{ci} \\ \frac{1}{2} \cdot A_i^{WT} \cdot \rho_{wind} \cdot Cp^{WT} \cdot V_r^3 \cdot \frac{V_{m,p}^{Env^2} - V_{ci}^2}{V_r^2 - V_{ci}^2}, & \forall V_{ci} \leq V_{m,p}^{Env} \cap V_{m,p}^{Env} \leq V_r \\ \frac{1}{2} \cdot A_i^{WT} \cdot \rho_{wind} \cdot Cp^{WT} \cdot V_r^3, & \forall V_r \leq V_{m,p}^{Env} \cap V_{m,p}^{Env} \leq V_{co} \end{cases} \quad (15)$$

Only one incentive policy can be selected, so the following constraint applies:

$$Y^{FIT} + Y^{NEM} \leq 1 \quad (8)$$

### 2.2.2. Design and capacity constraints

This section presents the design and capacity constraints for the various components of the microgrid: photovoltaic panel, wind turbine, biogas production, biogas electric generator, biogas heater, solar collector, thermal storage, electric shower, gas heater, air conditioning, and battery storage.

- Photovoltaic panel

The energy produced by the PV panel must not exceed its capacity:

$$E_{i,m,p}^{PV} \leq A_i^{PV} \cdot I_{t,m,p} \cdot ne_{i,m,p}^{PV} \cdot KL \quad (9)$$

where  $ne_{i,m,p}^{PV}$  is the time-dependent energy efficiency given by ([Karamov et al., 2021](#)):

$$ne_{i,m,p}^{PV} = nee^{PV} \cdot \left[ (1 - \beta_S) \cdot T_{m,p}^{SC} - 48 \right] \quad (10)$$

The operating temperature of the PV converter,  $T_{m,p}^{PV/SC}$  is:

$$T_{m,p}^{PV/SC} = T_{m,p}^{Env} + \frac{I_{t,m,p}}{K_0 + K_1 \cdot V_{m,p}^{Env}} \quad (11)$$

The PV energy generated must equal the sum of PV energy usage:

$$E_{i,m,p}^{PV} = E_{i,m,p}^{SELF,PV} + E_{i,m,p}^{SALE,PV} + \sum_j (E_{i,j,m,p}^{TRANSFER,PV} + E_{i,m,p}^{STORAGE,PV}) \quad (12)$$

The sale of PV electricity cannot exceed the electricity produced for consumption:

$$E_{i,m,p}^{SALE,PV} \leq E_{i,m,p}^{SELF,PV} + \sum_j (E_{i,m,p}^{TRANSFER,PV} + E_{i,m,p}^{STORAGE,PV}) \quad (13)$$

Due to space limitations, the total area allocated for PV panels and solar collectors must not exceed the available roof space:

$$A_i^{PV} + A_i^{SC} \leq PV_{up} \quad (14)$$

- Wind turbine

Electricity generation from the wind turbine depends on wind speed,  $V_{m,p}^{Env}$ , as follows ([Pallabazzer, 2003](#)):

The energy generated must equal consumption and storage needs:

$$E_{i,m,p}^{WT} = E_{i,m,p}^{SELF,WT} + E_{i,m,p}^{SALE,WT} + \sum_j (E_{i,m,p}^{TRANSFER,WT} + E_{i,m,p}^{STORAGE,WT}) \quad (16)$$

Wind turbine area is limited by available space:

$$A_i^{WT} \leq WT_{up} \cdot Y_i^{WT} \quad (17)$$

Similarly to the PV, the sale of WT electricity cannot exceed the electricity produced for consumption.

- Biogas production and usage

Total biogas production depends on the amount of organic matter available during the year:

$$Qbg = qb \bullet days \bullet months \sum_i (Qom_i + Qow_i) \quad (18)$$

The biogas production is given by:

$$Qbio_{i,m,p} = Qbgc_{i,m,p} + Qbgg_{i,m,p} + Qbhw_{i,m,p} \quad (19)$$

Biogas demand must be met for cooking food, electricity generation, and hot water generation:

$$Qbg = \sum_{i,m,p} Qbio_{i,m,p} \bullet h_p \bullet d_m \bullet s_m \quad (20)$$

Furthermore, due to local regulations ([NBR 13103, 2013](#)), the biogas production must be below 80 kW and will only be used if a pipeline exists.

The final volume of the biodigester is calculated according to [Otím et al. \(2006\)](#) and [Araujo \(2017\)](#), and will be considered 30 % larger than calculated due to the gaseous phase that will also be stored in it:

$$V^{BD} = \sum_i \frac{(Qom_i + Qow_i) \bullet IS}{DMO} \bullet tr \bullet (1 + 0.3) \quad (21)$$

Biogas generator energy output is constrained by its capacity:

$$E_{i,m,p}^{BG} \leq k_i^{BG} \bullet ne^{BG} \quad (22)$$

Moreover, biogas generator capacity must match the biogas production:

$$k_i^{BG} \leq Qbgg_{i,m,p} \bullet Hb \quad (23)$$

- Biogas heater

The energy output from the biogas heater is limited by biogas supply:

$$E_{i,m,p}^{BH} \leq Qbhw_{i,m,p} \bullet Hb \bullet ne^{BH} \quad (24)$$

Hot water generation is converted as follows:

$$E_{i,m,p}^{BH} = \frac{cp_{water} \bullet HW_{i,m,p}^{BH} \bullet \rho_{water} \bullet (T_{storage} - T_{m,p}^{Env})}{3600} \quad (25)$$

- Solar collectors and thermal storage

The energy collected by the solar collector is:

$$E_{i,m,p}^{SC} \leq A_i^{SC} \bullet It_{m,p} \bullet ne_{m,p}^{SC} \bullet KL \bullet Y_i^{SC} \quad (26)$$

Similarly to the case of the PV panel, the efficiency of the solar collector is expressed according to [Karamov et al. \(2021\)](#) as defined in [Eq. \(9\)](#).

Hot water produced is stored for later use:

$$HW_{i,m,p}^{SC} = HW_{i,m,p}^{STORAGE,SC} \quad (27)$$

Thermal storage energy balance is ([Sidnell et al., 2021a](#)):

$$HW_{i,m,p}^{TS} = (1 - \zeta) \bullet HW_{i,m,p-1}^{TS} + HW_{i,m,p}^{TS,in} - HW_{i,m,p}^{TS,out} \quad (28)$$

The energy removed from the system cannot be greater than the hot water that was loaded into the system:

$$HW_{i,m,p}^{TS,out} \leq (1 - \zeta) \bullet HW_{i,m,p-1}^{TS} \quad (29)$$

The stored volume cannot exceed tank capacity:

$$HW_{i,m,p}^{TS} \leq k_i^{TS} \quad (30)$$

- Electric shower

The electric shower must meet capacity constraints:

$$E_{i,m,p}^{ES} \leq k_i^{ES} \bullet ne^{ES} \quad (31)$$

- Gas heater

The gas heater's water output must be less than its capacity:

$$HW_{i,m,p}^{GH} \leq k_i^{GH} \quad (32)$$

- Air conditioning

The cooling capacity of air conditioning units is:

$$E_{i,m,p}^{AC} \leq k_i^{AC} \quad (33)$$

- Battery (electrical storage)

Energy storage dynamics in the battery are expressed by [Sidnell et al. \(2021a\)](#):

$$E_{i,m,p}^{STORAGE,BT} = (1 - \theta) \bullet E_{i,m,p-1}^{STORAGE,BT} + h_p \bullet (1 - X) \bullet E_{i,m,p}^{STORAGE IN,BT} - \frac{h_p \bullet E_{i,m,p}^{STORAGE OUT,BT}}{(1 - \Delta X)} \quad (34)$$

In addition, the battery charge must respect charge and discharge limits:

$$h_p \bullet (1 - X) \bullet E_{i,m,p}^{STORAGE IN,BT} \leq k_i^{BT} \bullet X_{up} \quad (35)$$

$$\frac{hours_p \bullet E_{i,m,p}^{STORAGE OUT,BT}}{(1 - \Delta X)} \leq k_i^{BT} \bullet \Delta X_{up} \quad (36)$$

Finally, the capacities of all technologies must be within capacity limits found in the market when the equipment is installed.

### 2.2.3. Demand equations

This section presents the material and energy resource balance to meet the demands for electricity, hot water, cooking gas and natural gas.

- General energy balance (for each resource  $r$ )

The energy demand for electricity, hot water, air conditioning, and cooking gas is met by self-generated resources (solar, wind, biogas, etc.), transfers between houses, and imports from the grid, with an additional storage component. For a resource  $r$  (electricity, hot water, etc.) this balance is determined as ([Sidnell et al., 2021a](#)):

$$\begin{aligned} Load_{i,m,p}^r &= \sum_j (\beta_{ij} \bullet E_{j,i,m,p}^{TRANSFER,r} - E_{i,j,m,p}^{TRANSFER,r}) \\ &= E_{i,m,p}^{GRID,r} + \sum_r E_{i,m,p}^{SELF,tech,r} + E_{i,m,p}^{STORAGE OUT,tech,r} \end{aligned} \quad (37)$$

- Energy transfer constraint (for each resource  $r$ )

The energy generated cannot be sold or transferred before the demand of the house is met, and this applies across all relevant resource types (electricity, hot water):

$$\sum_j (\beta_{ij} \bullet E_{j,i,m,p}^{TRANSFER,r} - E_{i,j,m,p}^{TRANSFER,r}) \leq E_{i,m,p}^{SELF,tech,r} + E_{i,m,p}^{STORAGE OUT,tech,r} \quad (38)$$

Additionally, specific cases for the air conditioning, cooking and natural gas must be considered:

$$Load_{i,m,p}^{AC} = E_{i,m,p}^{AC} \quad (39)$$

$$Load_{i,m,p}^C = G_{i,m,p}^{NG} + Qbgc_{i,j,m} \bullet Hb \quad (40)$$

$$Use_{i,m,p}^{NG} = G_{i,m,p}^{NG} + \frac{E_{i,m,p}^{GH}}{ne^{GH}} \quad (41)$$

#### 2.2.4. Operating constraints

In order to operate the network, some constraints must be imposed on the microgrid and the hot water pipeline.

- Microgrid

The sale of electricity generated by solar, wind, or biogas to the grid must not exceed a pre-defined maximum limit and cannot happen simultaneously with the purchase of electricity from the grid. This can be generalized into a single constraint that covers all sources, represented as  $E_{i,m,p}^{SALE,tech}$ :

$$\sum_r E_{i,m,p}^{SALE,tech} \leq Sale_{up} \bullet (1 - Y_{i,m,p}^{GRID}) \quad (42)$$

The electricity purchased from the grid cannot exceed the total demand of the house, including all relevant components:

$$E_{i,m,p}^{GRID} \leq \left( Load_{i,m,p}^E + \frac{Load_{i,m,p}^{AC}}{ACCOP} + \frac{E_{i,m,p}^{SELF,ES}}{ne^{ES}} \right) \bullet Y_{i,m,p}^{GRID} \quad (43)$$

Electricity cannot be transferred from house  $i$  to house  $j$  if house  $i$  is purchasing electricity from the central grid during the same time period:

$$E_{i,j,m,p}^{TRANSFER} \leq \left( Load_{i,m,p}^E + \frac{Load_{i,m,p}^{AC}}{ACCOP} + \frac{E_{i,m,p}^{SELF,ES}}{ne^{ES}} \right) \bullet (1 - Y_{i,m,p}^{GRID}) \quad (44)$$

The electricity transferred between houses is the sum of available electricity generated by various resources not used for self-consumption or grid sale:

$$E_{i,j,m,p}^{TRANSFER} = \sum_{res} E_{i,j,m,p}^{TRANSFER,r} \quad (45)$$

Electricity can only be transferred if there is a valid connection between houses, represented by the binary variable  $Y_{ij}^{MG}$ :

$$E_{i,j,m,p}^{TRANSFER} \leq \left( Load_{i,m,p}^E + \frac{Load_{i,m,p}^{AC}}{ACCOP} + \frac{E_{i,m,p}^{SELF,ES}}{ne^{ES}} \right) \bullet Y_{ij}^{MG} \quad (46)$$

To ensure one-directional transfer, house  $j$ 's electricity index must be higher than house  $i$ 's index when  $i$  is transferring electricity to  $j$ :

$$E_j \geq E_i + 1 - i \bullet (1 - Y_{ij}^{MG}) \quad (47)$$

Furthermore, no simultaneous transfers between a house  $i$  and another house  $j$  in both directions, nor any transfer within the same house are allowed:

$$\sum_j Y_{ij}^{MG} + \sum_j Y_{ji}^{MG} \leq 1 \quad (48)$$

$$Y_{i,i}^{MG} = 0 \quad (49)$$

$$E_{i,i,m,p}^{TRANSFER} = 0 \quad (50)$$

If a microgrid exists, the binary variable  $Z$  must indicate the existence of electricity connections between houses:

$$Z \geq Y_{ij}^{MG} \quad (51)$$

- Pipeline

The constraints for the hot water pipeline are similar to the microgrid constraints, but focus on hot water transfer instead of energy. Thus, hot water can only be transferred from house  $i$  to house  $j$ , but not in the reverse direction, and no house can transfer and receive hot water simultaneously.

House  $j$  must have higher hot water index than house  $i$  when  $i$  is transferring hot water to  $j$ :

$$O_j \geq O_i + 1 - i \bullet (1 - Y_{ij}^P) \quad (52)$$

In terms of the hot water transferred between houses, this will be equal to the sum of available hot water generated by different sources (gas heater, biogas heater, thermal storage, etc.):

$$HW_{i,j,m,p}^{TRANSFER} = \sum_{tech} HW_{i,j,m,p}^{TRANSFER,tech} \quad (53)$$

Furthermore, no hot water transfer within the same house is allowed, and transfer can only happen if there is a valid pipeline between houses, represented by a binary variable  $Y_{ij}^P$ . A final set of constraints are imposed due to the limited space available within households. In this case, a house can only have either a biogas heater or a natural gas boiler, but not both.

#### 2.3. Model implementation

The model presented in the previous section includes three nonlinear equations, Eqs. (5), (6) and (25), along with linear equations, and involves both discrete and continuous variables. This formulation results in a Mixed-Integer Nonlinear Programming (MINLP) problem.

The mathematical formulation of the problem is:

$$\begin{aligned} \min \quad & C_{TOTAL}(\mathbf{x}, \mathbf{y}) \\ \text{s.t. } & \mathbf{x}, \mathbf{y} \in \Omega \\ \Omega = \{ & \mathbf{x} \in \mathbb{R}^N, \mathbf{y} \in \mathbb{Z}^N \mid g_i(\mathbf{y}) \geq 0, i = 1, \dots, s, h_i(\mathbf{x}, \mathbf{y}) \geq 0, i \\ & = 1, \dots, m, h_i(\mathbf{x}) = 0, i = 1, \dots, p \} \end{aligned} \quad (55)$$

Here  $C_{TOTAL}$  is the objective function,  $x$  and  $y$  are the continuous and binary decision variables respectively, subject to the set of constraints  $\Omega$ .

The resulting MINLP problem is implemented in the General Algebraic Modelling System (GAMS) software ([GAMS, 2021](#)) and solved using the Branch-And-Reduce Optimization Navigator (BARON) solver ([Tawarmalani, Sahinidis, 2005; Sahinidis, 2021](#)), which can handle a wide range of MINLP problems, including those with nonlinear equations, discrete variables, and multiple local optima. Upper and lower bound values were applied to all decision variables.

#### 2.4. Case study

The selected site is the city of Salvador, Bahia, Brazil. The country currently incentivizes renewable energy through Net Metering policy, and this study evaluates whether this option remains viable across different scenarios. However, Brazil lacks a well-defined carbon pricing system. To estimate environmental costs, this case study references countries like the UK, which uses a carbon tax of R\$0.12/kg CO<sub>2</sub> ([Sidnell](#)

et al., 2021a) based on an exchange rate of R\$6.58/£. Given Brazil's GDP is approximately half of the UK's, the carbon tax is adjusted to R \$0.06/kg CO<sub>2</sub>. Additionally, the capital recovery factor was calculated using an interest rate of 7 % over 20 years.

The model's resource limits were set based on local constraints, market capacity, and regulations. Fixed costs were estimated from studies like Mustafa (2010), and variable costs were derived from fuel or water prices when generating hot water. These parameters are detailed in the [Supplementary Material](#).

The model considered electricity, cooling, hot water, and gas for cooking as demands. Since no studies on post-COVID Brazilian energy demand were found, electricity demand was assumed 25 % higher with continuous usage throughout the day, reflecting the rise in remote work (Macedo, 2001). Hot water demand increased by 15 %, cooling demand by 50 %, and cooking gas by 25 %. Fig. 2 shows electricity and hot-water demand profiles for pre- and post-COVID scenarios. Each household's consumption depends on factors like the number of residents and lifestyle, so demand variations were applied by scaling the average values shown in Fig. 2 using the multipliers in Tables 2 and 3.

Electricity rates follow Brazil's system (Neoenergia Coelba, 2020): peak (18:00 – 20:59), intermediate (16:00 – 17:59) and off-peak hours (remaining times). In the post-COVID scenario, electricity rates increase by 15 % during peak hours, 10 % during off-peak hours, and 16 % during intermediate hours, respectively, due to greater grid usage during the pandemic. A similar trend is observed in natural gas prices.

### 3. Results

In this section, the results of the optimization study are presented, starting with a discussion of the time-horizon splitting methods and followed by the optimal grid configurations for different scenarios. The study highlights the advantages of clustering methods for time-horizon discretization, the importance of accounting for time-dependent efficiency profiles, and the resilience of the proposed microgrid design across varying demand profiles (pre- and post-COVID) and different numbers of households.

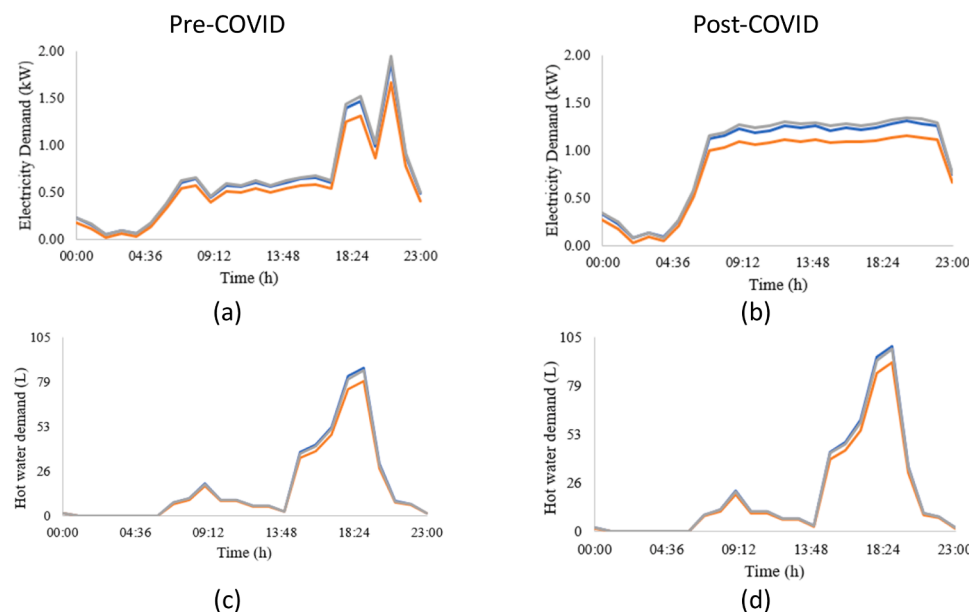


**Fig. 2.** Average energy demand in Salvador, Brazil in the pre- and post-COVID scenarios for: (a-b) electrical demand (kW); (c-d) hot water (L). Source: EPE (2018); EPE (2021).

**Table 2**

Scalars to estimate the demand for each house.

Houses	Scalar
i1, i6	0.2
i2, i7	0.6
i3, i8	1.0
i4, i9	1.4
i5, i10	1.8

### 3.1. Splitting the

#### 3.1.1. time horizon

To discretize the time horizon for the optimization problem, both empirical and clustering methods were applied to data on electricity demand, solar irradiation, wind speed, and electricity prices (Fig. 3). Using the empirical method for the pre-COVID scenarios, the year was divided into two seasons ( $m = 2$ ) and seven periods of varying durations ( $p = 7$ ).

For the clustering method, applied to both pre- and post-COVID scenarios, the elbow method was used to determine the optimal number of clusters. In the pre-COVID scenario, the data for solar irradiation, wind speed and electricity demand were normalized, and three clusters were identified (Fig. 4a), resulting in three seasons ( $m = 3$ ). These seasons were then divided according to electricity rates, and the elbow method was again applied to identify time periods during the day. Initially, the clustering did not produce consecutive time periods, so additional clusters were tested until eight consecutive periods ( $p = 8$ ) were identified, as shown in Fig. 4b. The final time period distribution for the pre-COVID scenario is illustrated in Fig. 5, with  $m = 3$  and  $p = 8$ .

### 3.2. Microgrid optimization

The capacity of the MINLP optimization model was tested with five and ten houses, exploring the influence of various factors on the microgrid design: i) time-dependent profiles for wind and photovoltaic generation efficiencies; ii) time horizon discretization methods; iii) number of houses; and iv) demand profile. Three scenarios were considered to evaluate these influences:

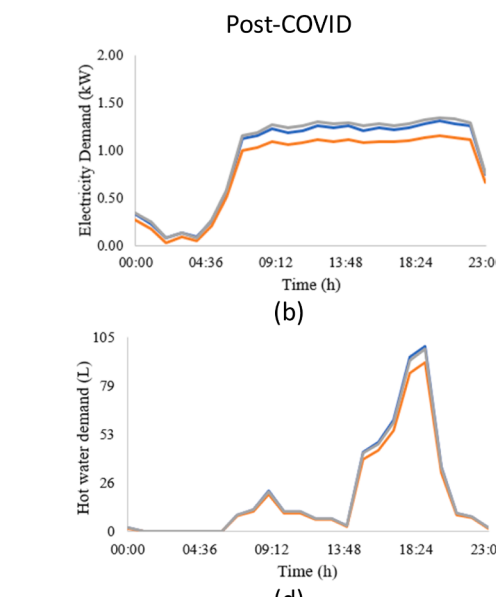


**Table 3**

Results for the scenarios with energy resources distributed at a 0 % gap.

Stage	Scenario	Houses	Single equations	Single variables	Discrete variables	CPU time (s)	Objective Function (R\$)
Pre-COVID	S1	5	12,203	8504	224	263.93	10,261.60
	S3	5	6895	5096	174	59.64	52,458.11
	S2	5	11,100	8576	224	968.59	28,956.95
	S2	10	31,770	24,321	544	446,850.31	50,434.78
Post-COVID	S2	5	7023	5444	179	164.23	31,596.10
	S2	10	20,043	15,384	454	71,306.31	50,370.09

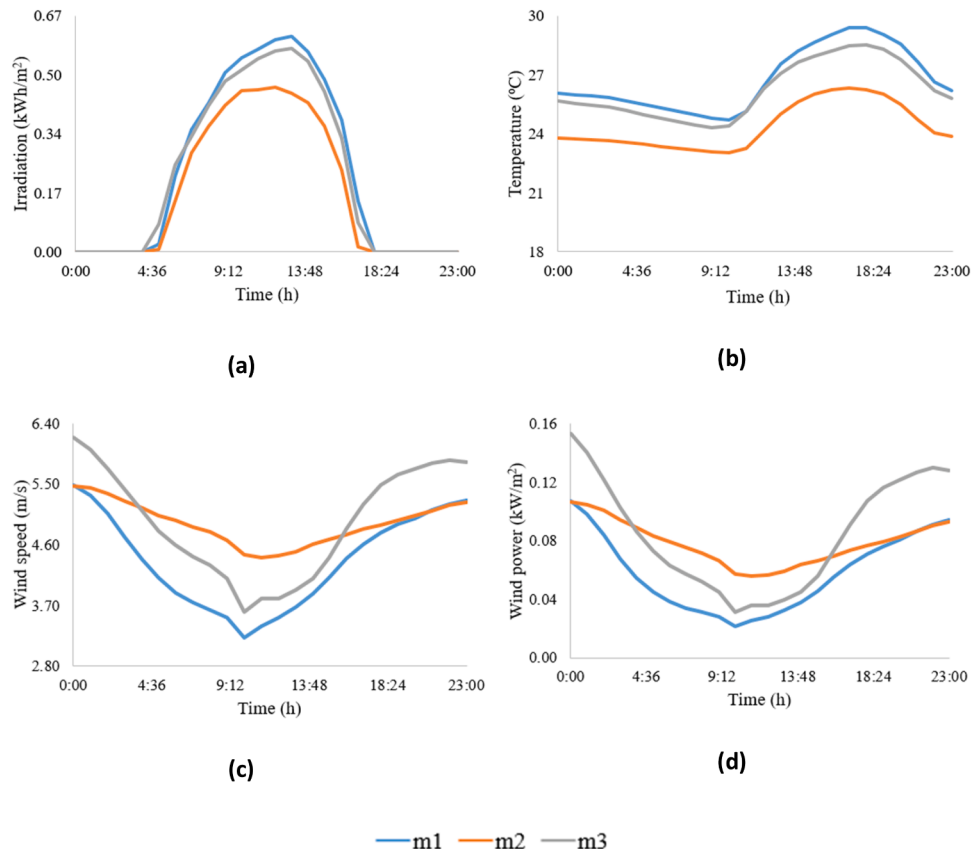


Fig. 3. Local conditions: (a) Solar irradiation; (b) Temperature; (c) Wind speed; (d) Wind power. Source: [World Bank Group \(2022\)](#); [DTU Wind Energy \(2022\)](#).

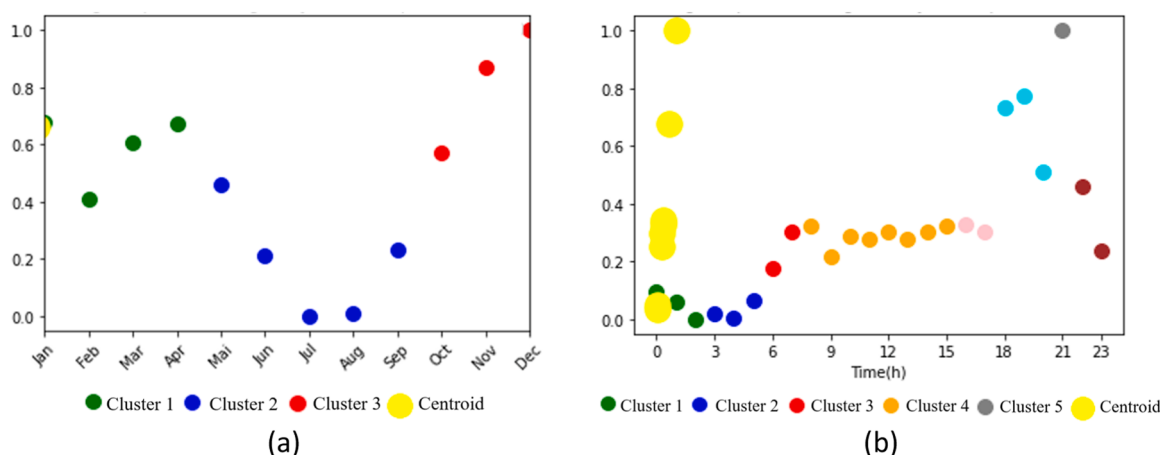


Fig. 4. Clustering the period (a) during the year and (b) during the day in the pre-COVID scenario.

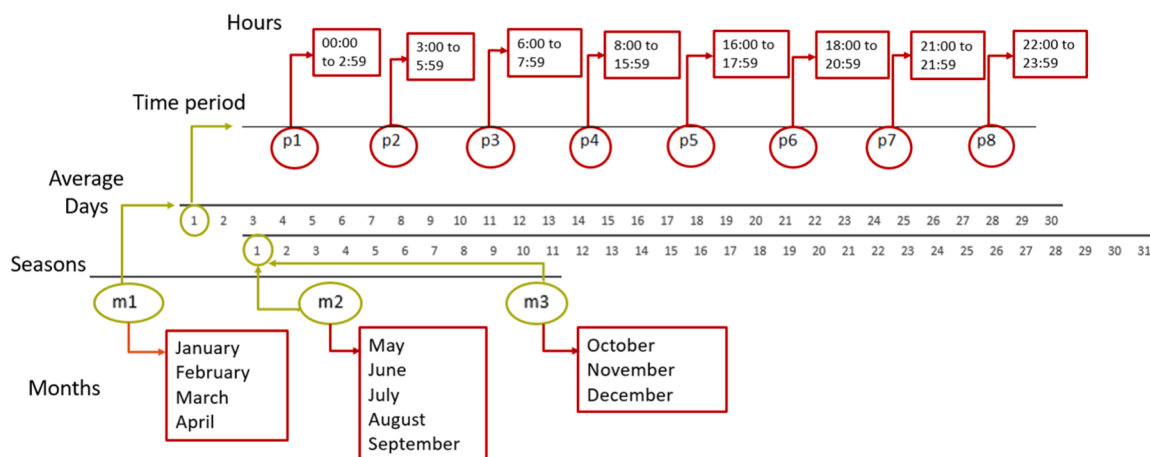


Fig. 5. Time period during the year for the pre-COVID scenario.

Table 4

Size of renewable resources for scenarios S2 (pre- and post-COVID) and S3<sup>[1]</sup>.

Scenario	Houses	Natural Gas Heater (L)	Biogas Heater (L)	Solar collector (m <sup>2</sup> )	Solar Tank (L)	Air Conditioning (kW)	Wind Turbine (m <sup>2</sup> )	PV Panel (m <sup>2</sup> )	Battery (kW)
S2 (clustering) Pre-COVID <sup>[2]</sup>	1	400.00	-	6.54	200.00	2.20	2.74	2.60	4.22
	2	400.00	-	11.16	200.00	2.20	-	12.20	10.23
	3	400.00	-	19.70	200.00	2.20	5.00	16.56	15.16
	4	400.00	-	13.02	200.00	2.20	-	22.26	-
	5	-	400.00	16.74	200.00	2.21	5.00	26.29	-
S2 (clustering) Post-COVID <sup>[2]</sup>	1	400.00	-	3.67	200.00	2.20	4.83	4.48	2.73
	2	-	-	-	-	2.20	-	25.67	19.45
	3	400.00	-	1.43	200.00	3.31	5.00	34.18	20.35
	4	-	400.00	-	-	4.63	-	39.77	-
	5	400.00	-	-	-	5.96	5.00	48.95	-
S3 (empirical) Pre-COVID <sup>[2]</sup>	1	-	400.00	5.62	200.00	2.20	5.00	2.06	5.93
	2	400.00	-	10.66	200.00	2.20	-	17.63	9.92
	3	400.00	-	18.57	232.99	3.46	5.00	45.97	46.32
	4	400.00	-	12.44	200.00	4.84	-	20.24	-
	5	-	400.00	15.99	200.27	6.22	5.00	22.56	-

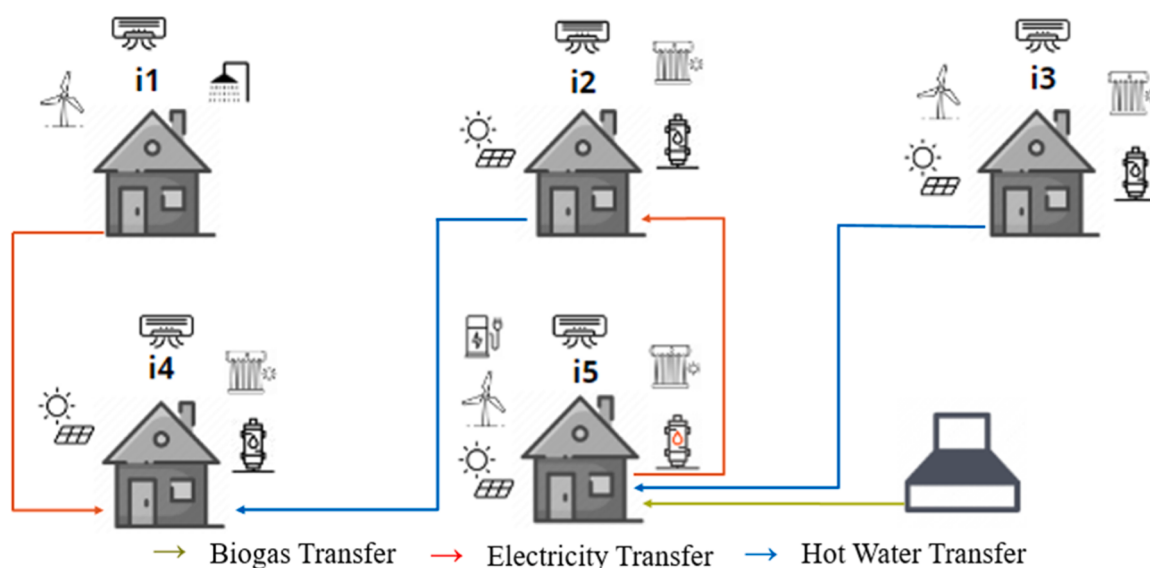
<sup>[1]</sup>Electric shower was only installed in house i2 in S2 post-COVID, therefore no other source of hot-water was selected.<sup>[2]</sup>Biodigester: 0.84 m<sup>3</sup> and no extra organic material purchased by the microgrid (S2 pre-COVID); 1.48 m<sup>3</sup> of biogas and 12.72 kg/day of purchased biomass (S2 post-COVID); 0.86 m<sup>3</sup> of biogas and 0.76 kg/day of purchased biomass (S3 pre-COVID).

Fig. 6. Optimal energy resources and connections between houses for S1 during pre-COVID for five houses: time-constant efficiency profiles of the solar panel, solar collector and wind turbine and clustering to split the time domain.

- **Scenario 1 (S1):** Time-constant efficiency profiles for solar panels, solar collectors, and wind turbines, with the *clustering* method to discretize the time horizon.
- **Scenario 2 (S2):** Time-dependent efficiency profiles for solar panels, solar collectors, and wind turbines, with *clustering* method to discretize the time horizon.
- **Scenario 3 (S3):** Time-dependent efficiency profiles for solar panels, solar collectors and wind turbines, but using the *empirical* method to discretize the time horizon.

Each scenario was compared to a baseline where no distributed energy resources were installed, and electricity was supplied solely by the central grid. For scenarios S1 and S2, the baseline is identical, while S3 has a different baseline due to differences in time-discretization methods.

Results for the scenarios with five and ten houses, obtained using GAMS Studio 0.8.6 for an optimality gap of 0 % on an Intel(R) Core(TM) i9-9900K CPU 3.60 GHz, are shown in Table 4. The complexity of the problem increases with the number of houses, leading to a significant rise in computational time, particularly for scenario S2, where the clustering method increased the number of equations due to a higher number of season and periods. For example, moving from five to ten

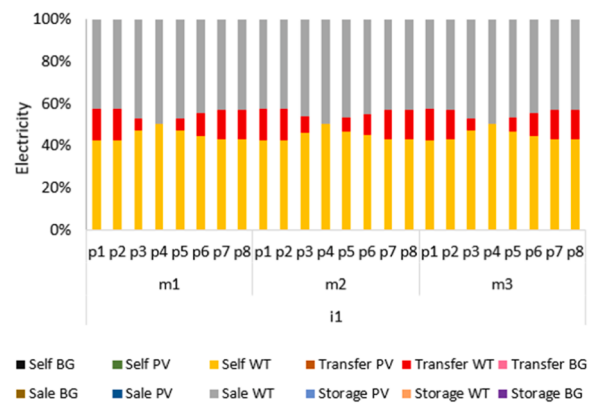


Fig. 8. Distribution of electricity generation in house i1 by distributed renewable resources for Scenario 1 pre-COVID for a microgrid with 5 houses.

houses in S2 increased the CPU time by over 124 hours in CPU time.

### 3.2.1. The effect of time-dependent efficiencies

The optimal configuration of S1 is illustrated in Fig. 6, with

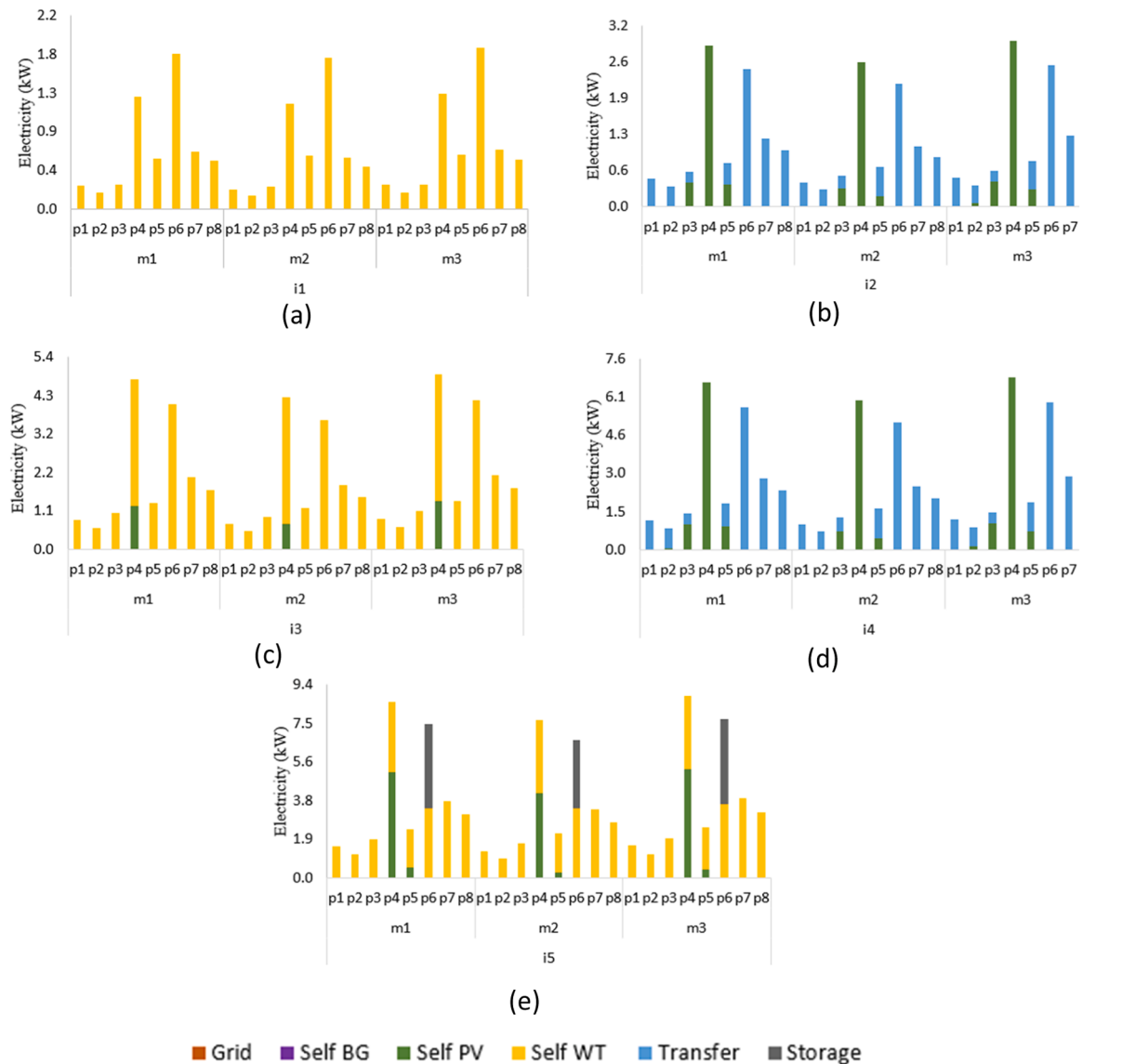
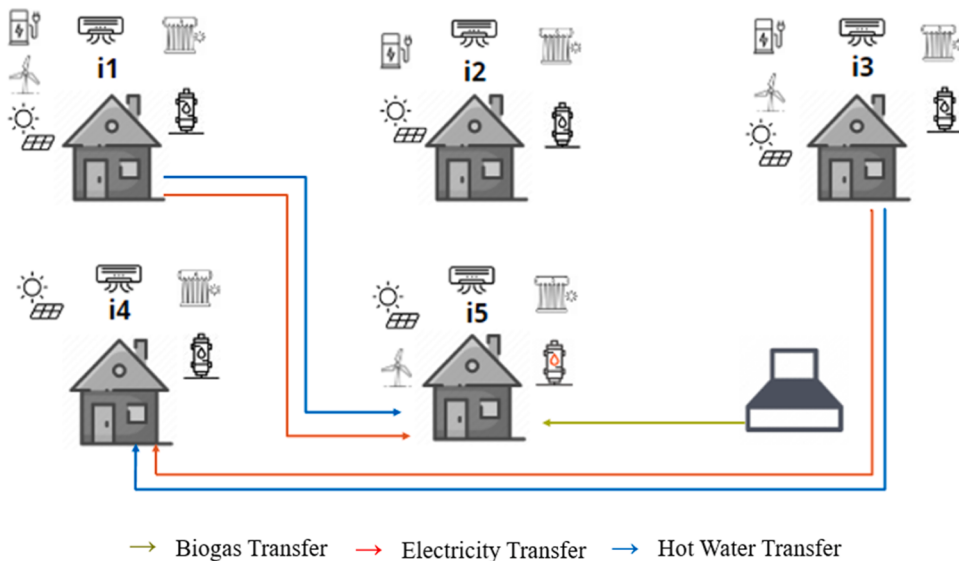
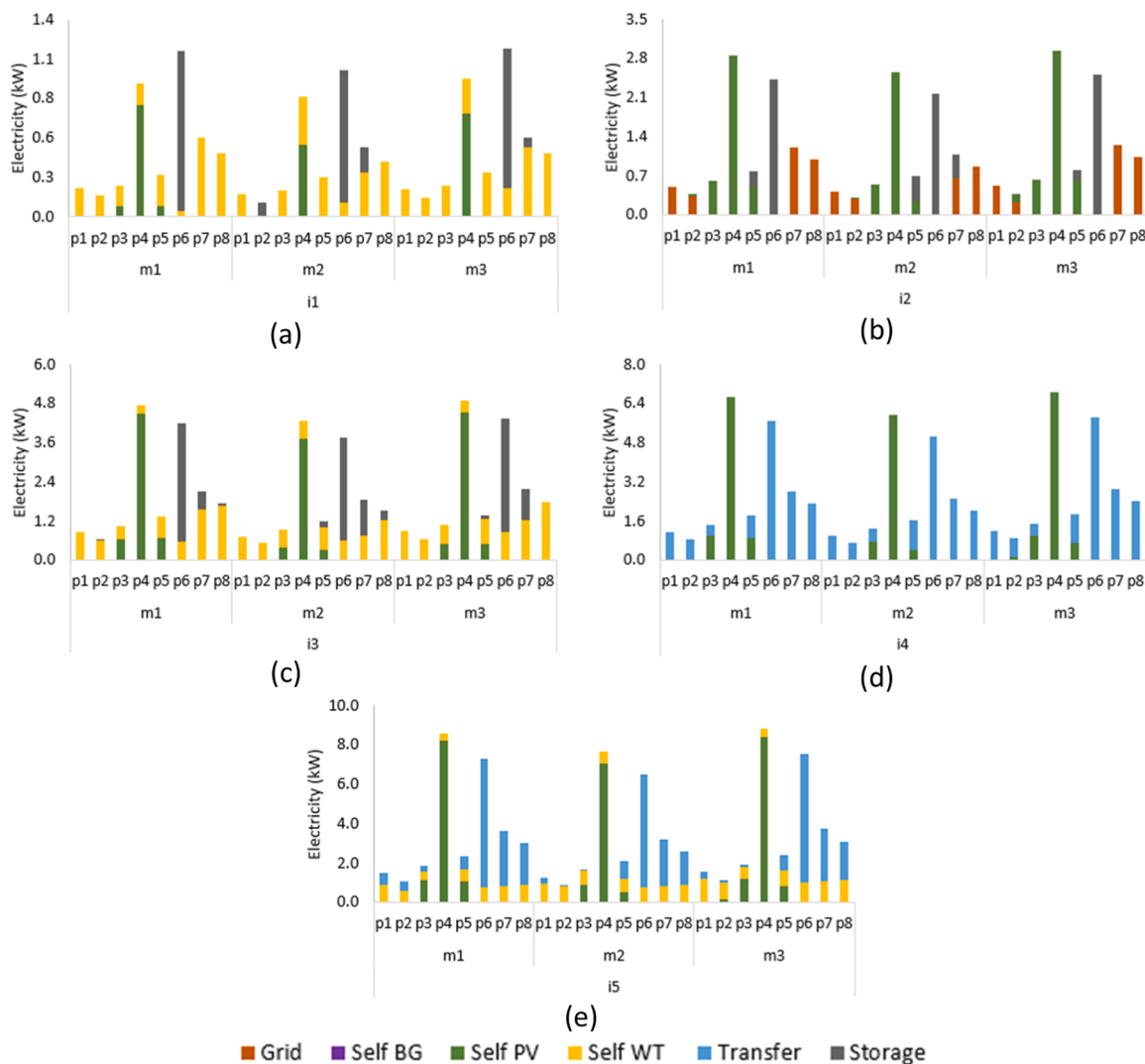


Fig. 7. Profile of resources used to meet the electrical demand in S1 pre-COVID for a microgrid with 5 houses: a) i1; b) i2; c) i3; d) i4; e) i5.



**Fig. 9.** Optimal energy resources and connections between houses for S2 during pre-COVID for five houses: time-dependent efficiency profiles of the solar panel, solar collector and wind turbine and clustering to discretize the time domain.



**Fig. 10.** Profile of resources used to meet the electrical demand in S2 pre-COVID for a microgrid with 5 houses: a) i1; b) i2; c) i3; d) i4; e) i5.

corresponding resource profiles shown in Fig. 7. In S1, air conditioning is installed in all houses to meet the cooling demand. The wind turbine is preferred for electric energy, with houses i1, i3 and i5 adopting it.

Notably, the optimization prohibits neighboring houses from having wind turbines, leading houses i2 and i4 to meet their demand mainly through energy transfers. House i1 shares 15 % of its generated electricity with house i4 and sells about 40 % to the central grid (Fig. 8). All houses except i1 have PV panels, with i1 having the lowest demand. Houses i2 and i4 produce solar energy when available (p2 to p6) and rely on the microgrid otherwise. A battery is installed only in house i5, which has the highest demand, storing energy during lower demand periods.

For hot water demand, house i1 uses an electric shower due to its lower demand, while other houses use a solar collector with a natural gas (i2, i3, i4) or biogas heater (i5). Houses i4 and i5, having higher hot water demands, receive hot water from houses i2 and i3, respectively. The results suggest that transferring hot water from another house is preferable to installing larger equipment in the residence.

Scenario S1's time-constant efficiencies led to an overestimated energy generation. Considering time-dependent profiles in S2 (Fig. 9) resulted in a more realistic scenario. In S2, batteries were installed in houses i1, i2 and i3, and house i1 had also a PV panel. During the peak solar period (p4), PV was used preferentially (Fig. 10), and surplus energy was stored for transfer to house i5. House i2 did not transfer energy or hot water, but it consumed from the central grid during off peak periods. Stored energy was used during peak periods (p6) instead of grid energy, with batteries providing an optimal solution. In S1, the wind turbine alone could meet house i1's self-demand, but in S2, time-varying efficiencies led to the installation of additional technologies, including PV panels and batteries, confirming that neglecting time-varying efficiencies leads to overestimated energy generation.

Hot-water demand in S2 is met by solar collectors, and a biogas heater was installed in house i5 due to its higher demand. A biodigester with a volume of  $0.84 \text{ m}^3$  supplies biogas for hot water and cooking in house i5, while other houses use natural gas due to lower demand (Fig. 11). The capacity of the resources installed in each house is summarized in Table 4. The choice of biogas over natural gas in house i5 is attributed to its lower cost and higher hot water demand. However, the limited biogas production necessitates additional hot water transfers from house i1. Cooking gas demand is mostly met by natural gas, as biogas is predominantly used for heating water.

### 3.2.2. The effect of clustering method for splitting the time horizon

Fig. 12 compares the resource profiles of house i1 in S2 (clustering method) and S3 (empirical method). In both scenarios, house i1 transfers energy to houses i5. The results indicate that the clustering (S2) allows for more efficient use of solar panels and batteries compared to the empirical method (S3), despite similar dimensions as Table 4 shows.

Resources installed in S2 and S3 (pre-COVID) were comparable, but the PV panels in houses i2 and i3 and the battery in i3 were significantly

larger in S3, impacting the overall cost. The total cost for S2 is R\$ 28,956.95, while for S3 it was R\$ 52,458.11 (Table 5). This highlights the effectiveness of the clustering method in optimizing the installed resources.

### 3.2.3. Demand profile: pre- and post-COVID

The post-COVID scenario imposed a 25 % increase in electricity demand and a 50 % increase in air cooling demand. The optimal configuration in S2 (time-dependent efficiencies and clustering) remained similar to Fig. 9 but included a biodigester in house i4 due to increased consumption and limited biogas production (Table 4).

Hot water demand for houses i4 and i5 was met through transfers from i1 and i3, with solar collectors and natural gas heaters supplementing the needs. In the post-COVID scenario, house i2, not sharing electricity or hot-water, sold energy to the central grid and received credits from net metering (Fig. 13). During periods p2 and p3, house i2 fed 40 %–50 % of generated energy into the grid and used stored energy or grid supply after sunset. The electric shower in house i2 required a larger PV panel and battery compared to pre-COVID. Despite increased demand, the total microgrid cost rose by only 9 % with respect to the pre-COVID scenario due to a 125 % increase in net metering credits, as Table 5 shows.

### 3.2.4. Number of houses

The model formulation was extended to a microgrid with ten houses. Compared to the five-house scenario (Fig. 9), the ten-house configuration altered energy and thermal sharing dynamics (Fig. 14). House i6, instead of i5, generated hot water using a biogas heater, and shared biogas with house i5. This result suggests that smaller capacity water heater units in each house are more feasible than a larger unit in a single house.

Fig. 15a shows resource profiles for meeting house i6's hot water demand. Limited biogas production required additional solar collectors. The biogas transferred to i5 was primarily used for cooking, but due to its low availability (Fig. 15b), additional organic material purchases were not cost-effective. This indicates that larger biodigesters could be beneficial in rural microgrids with more organic production.

### 3.2.5. Overall comparison

Table 5 summarizes the costs and revenues for the scenarios discussed. The baseline (B) represents the costs relying solely on the central grid. Scenarios S1 and S2 have the same baseline, but differences emerge when the empirical method (S3) or varying number of houses are considered.

The net metering, the current incentive in Brazil, plays a significant role in reducing costs. Renewable resources reduce grid costs and natural gas usage, with the policy substantially lowering the total cost.

While renewable investments increase initial costs, savings from reduced grid purchases and net metering credits are crucial for

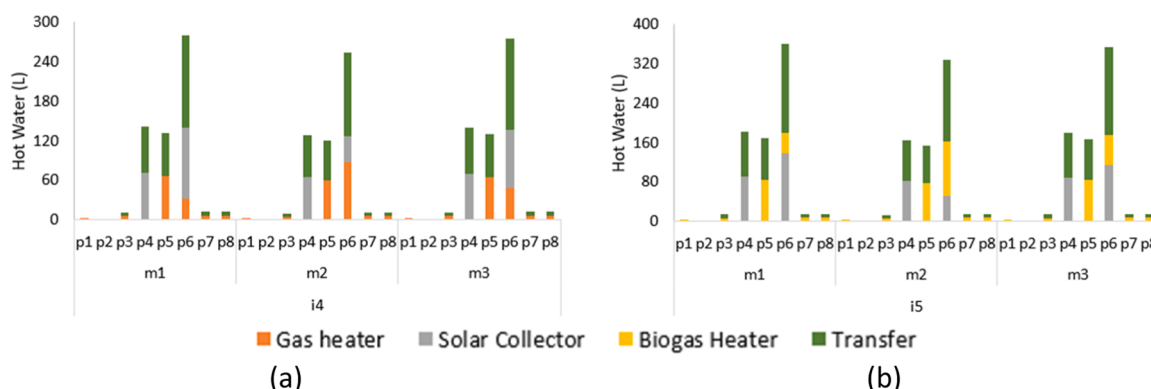
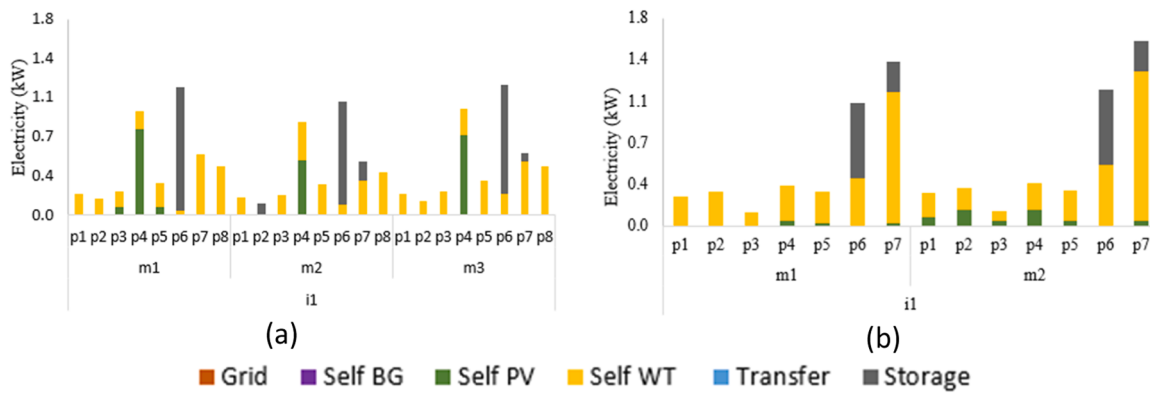


Fig. 11. Profile of resources used to meet the hot water demand in S2 pre-COVID for a microgrid with 5 houses: a) i4; b) i5.



**Fig. 12.** Profile of resources used to meet the electrical demand in house i1 according to the method for splitting the time horizon: a) S2 (clustering method) and b) S3 (empirical method).

**Table 5**  
Costs and revenues for all scenarios<sup>[1]</sup>.

#	Houses	Total Cost (R \$)	Investment (R \$)	O&M Cost (R \$)	Grid Energy Cost (R\$)	Natural Gas Cost (R\$)	Environmental Total Cost (R\$)	PV - Net Metering	WT - Net Metering
<b>Pre-COVID</b>									
B	5	160,210.26	990.15	84,672.04	68,722.25	3809.99	2015.82	-	-
S1	5	10,261.60	18,090.40	39,108.92	-	2557.95	1256.69	20,680.62	30,071.75
S2	5	28,956.95	24,450.86	38,539.39	845.82	2599.89	1428.47	31,004.54	7902.94
B	5	154,151.17	1430.53	66,499.38	83,043.32	1766.99	1410.94	-	-
S3	5	52,458.11	32,224.66	33,506.08	4139.58	693.10	554.72	11,640.61	7019.43
B	10	320,420.51	1980.30	169,344.09	137,444.50	7619.99	4031.64	-	-
S2	10	50,434.78	47,079.12	70,171.55	1117.29	5122.33	2846.50	62,623.51	13,278.50
<b>Post-COVID</b>									
B	5	249,889.14	1398.02	109,351.27	128,398.45	7595.89	3145.50	-	-
S2	5	31,596.10	28,056.46	80,756.17	1755.81	5985.75	2562.79	77,561.29	9959.60
B	10	499,757.41	2775.18	218,702.54	256,796.90	15,191.78	6291.01	-	-
S2	10	50,370.09	51,037.36	146,725.13	2637.08	12,629.48	5176.71	153,671.66	14,164.02

[1]B: Baseline scenario for each time

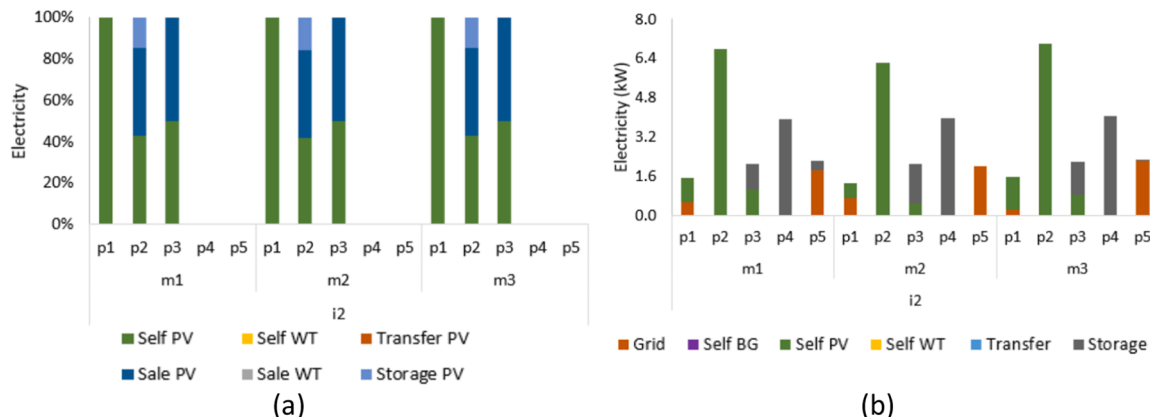


**Fig. 13.** Distribution of electricity generation (a) and profile of resources (b) used to meet the electrical demand in house i2 for S2 during post-COVID.

microgrid feasibility. Neglecting time-varying efficiencies (S1) results in an overestimation of energy generation, increasing costs threefold compared to a realistic scenario (S2). The clustering method (S2) was 45 % more cost-effective than the empirical method (S3). Despite higher post-COVID demands, optimization ensured only a 9 % increase in total cost, demonstrating the balance between investment and net metering benefits.

#### 4. Conclusions

This study aimed to address gaps in the modeling of distributed

energy systems by exploring the impact of incentive policies and time-dependent efficiencies of renewable resources. Despite the nonlinearity introduced by time-dependent efficiencies, the MINLP framework effectively optimized microgrid configurations across various scenarios for up to ten houses. The choice of incentive policy was crucial, as the model shows that credits from mechanisms like net metering significantly are offsetting the higher investment required for renewable technologies.

Accounting for time-dependent efficiencies was essential for accurate microgrid design. Neglecting these variations often led to an overestimation in the capacity of installed technologies, adversely affecting

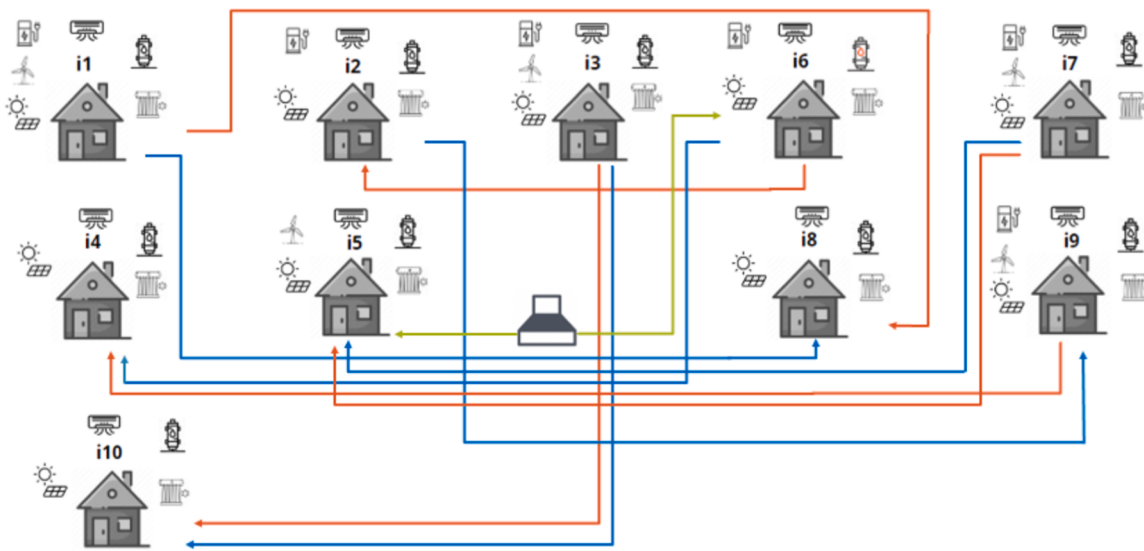


**Fig. 14.** Diagram of energy resources and connections between houses for the microgrid with 10 houses for Scenario 2 pre-COVID.

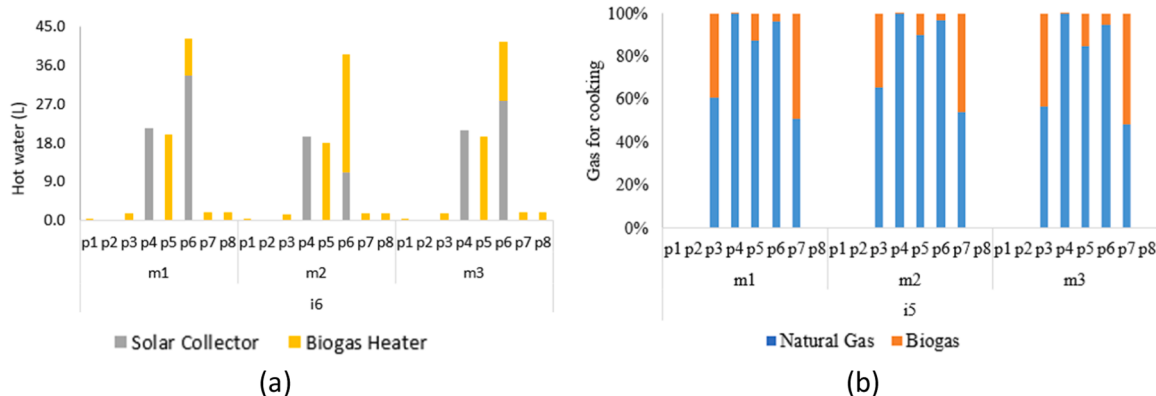


**Fig. 15.** Profile of resources used to meet the hot-water demand (a) and share of renewable resources to meet cooking gas demand during the pre-COVID S2 in a microgrid with 10 houses.

microgrid performance in real-world applications. A clustering method for discretizing the time horizon resulted in a 45 % reduction in total microgrid cost, due to more efficient utilization of renewable resources, minimizing equipment investments, and maximizing the benefits of net metering credits.

The feasibility of incorporating biogas into the microgrid was confirmed across all scenarios, although its use was limited by the availability of biomass waste. Biogas remains a competitive option compared to natural gas if provided on a larger scale by the central grid, particularly in rural settings. Additionally, solar thermal energy proved to be a viable alternative to gas heaters for hot water production, with solar collectors being installed in all scenarios, either in individual houses or for shared use.

The study also highlighted the advantages of microgrid synergies, demonstrating that it is more cost-effective to install multiple technologies and share energy within the microgrid than to invest in larger equipment for individual houses with higher demand. This approach enhances overall profitability and efficiency, underlining the importance of integrating various technologies and leveraging shared resources in microgrid systems.

The small-scale design, involving microgrids of up to ten houses, served as a proof of concept, aligning with comparable literature to demonstrate framework feasibility. Scaling the framework for larger groups would require addressing several factors:

- Computational complexity: increasing the number of houses would significantly expand the optimization problem and computational demands. Technique like decomposition methods, parallel computing, or simplified surrogate models could address this challenge while retaining system fidelity.
- Economic and ecological impact: larger studies would yield greater impact in terms of energy savings, emissions reduction, and overall sustainability. Economies of scale are expected in both operational and environmental benefits. Expanding the model to incorporate localized resources data would improve real-world applicability.
- Grid integration and management: a larger scale would necessitate advanced load management, storage and grid interaction strategies. Enhanced modeling for grid support and energy trading would likely improve both economic and ecological performance.

The following measures could extend this study to larger scales:

- Incorporating region-specific data on renewable resources, energy demand, and grid conditions to enhance model accuracy
- Conducting sensitivity analyses and uncertainty quantification to ensure robust system designs under diverse scenarios, including policy changes or shifts in resource availability.

To further refine and enhance the model and its results, several

avenues for future research can be pursued. First, integrating a broader range of renewable technologies and energy storage options could provide a more comprehensive assessment of their interactions and benefits. For example, including advancements in energy storage systems like solid-state batteries or exploring the potential of hydrogen as an energy carrier could offer new insights into optimizing microgrid configurations.

Secondly, incorporating real-time data and dynamic weather forecasting into the optimization model could improve the accuracy of time-dependent efficiencies and energy predictions. This would enable more responsive and adaptive microgrid operations, particularly in addressing the variability of renewable resources.

Further model extensions could explicitly incorporate uncertainty analysis, such as scenario-based or stochastic programming approaches, to enhance operational robustness. Although these methods increase problem size and computational complexity, as noted in (De Mel et al., 2023), advanced optimization techniques such as metaheuristic algorithms, hierarchical or multi-level optimization, or hybrid methods could potentially facilitate handling of larger-scale problems with greater efficiency. These techniques may offer improved computational performance and solution quality, especially as the size and complexity of the microgrid increase.

Lastly, investigating the economic and social impacts of different incentive policies on microgrid adoption and performance could provide valuable insights. Understanding how policy changes affect both the feasibility and acceptance of renewable technologies would contribute to more effective and equitable energy solutions.

#### CRediT authorship contribution statement

**Karen Pontes:** Writing – review & editing, Writing – original draft, Supervision, Software, Resources, Project administration, Methodology, Funding acquisition, Conceptualization. **Ana Paula Alves Amorim:** Writing – original draft, Visualization, Validation, Methodology, Investigation, Data curation. **Harvey Arellano-Garcia:** Writing – review & editing, Supervision, Resources, Project administration, Funding acquisition, Conceptualization. **Bogdan Dorneanu:** Writing – review & editing, Writing – original draft, Visualization, Validation, Supervision, Software, Methodology, Investigation, Formal analysis, Conceptualization.

#### Declaration of Competing Interest

The authors declare that they have no known competing financial interests or personal relationships that could have appeared to influence the work reported in this paper.

The author is an Editorial Board Member/Editor-in-Chief/Associate Editor/Guest Editor for [Journal name] and was not involved in the editorial review or the decision to publish this article.

#### Acknowledgment

The authors thank the Coordination for the Improvement of Higher Education Personnel – Brazil (CAPES) – Finance Code 001, the Foundation for Research Support of the State of Bahia (FAPESB) and the National Council for Scientific and Technological Development (CNPq) for the financial support.

#### Appendix A. Supporting information

Supplementary data associated with this article can be found in the online version at doi:10.1016/j.cherd.2024.12.033.

#### References

- Abgd – Associação Brasileira de Geração Distribuída. Geração própria de energia atinge 30 GW no Brasil, 2024. Available at: <https://www.abgd.com.br/portal/geracao-própria-de-energia-atinge-30-gw-no-brasil/#:-:text=Respons%C3%A1vel%20 pelo%20abastecimento%20de%20mais,e%20a%20descarboniza%C3%A7%C3%A3o%20 da%20ind%C3%A3stria>. Last accessed on September, 23rd, 2024.
- Absolar. Energia Solar Fotovoltaica no Brasil infográfico ABSOLAR. São Paulo: Associação Brasileira de Energia Solar Fotovoltaica, 2024. Available at: <https://www.absolar.org.br/mercado/infografico/>. Last accessed on September, 23rd, 2024.
- Agência Brasil. Capacidade de geração de energia eólica deve bater recorde neste ano, 2023. Available at: <https://agenciabrasil.ebc.com.br/economia/noticia/2023-04/capacidade-de-geracao-de-energia-eolica-deve-bater-recorde-neste-ano#:~:text=De%20acordo%20com%20a%20Associa%C3%A7%C3%A3o,energia%20que%2020pa%C3%A9s%20precisa>. Last accessed on September, 23rd, 2024.
- Araujo, Ana Paula Caixeta. Produção de biogás a partir de resíduos orgânicos utilizando biodigestor anaeróbico. 42 f. TCC (Bachelor) – Curso de Engenharia de Engenharia Química. Universidade Federal de Uberlândia, Uberlândia, 2017.
- Chinthavali, Supriya, Tansakul, Varisara, Lee, Sangkeun, Whitehead, Matthew, Tabassum, Anika, Bhandari, Mahabir, Munk, Jeff, Zandi, Helia, Buckberry, Heather, Kuruganti, Teja, Hill, Justin, Cortner, Chase, 2022. COVID-19 pandemic ramifications on residential Smart homes energy use load profiles. Energy Build. v. 259. <https://doi.org/10.1016/j.enbuild.2022.111847>.
- Clarke, Fiona, DORNEANU, Bogdan, MECHLERI, Evgenia, ARELLANO-GARCIA, Harvey, nov. 2021. Optimal design of heating and cooling pipeline networks for residential distributed energy resource systems. In: Energy, [S.L], v. 235. Elsevier BV, 121430. <https://doi.org/10.1016/j.energy.2021.121430>.
- De Mel, I., Demis, P., Dorneanu, B., Klymenko, O.V., Mechleri, E.D., Arellano-Garcia, H., 2023. Global sensitivity analysis for design and operation of distributed energy systems: a two-stage approach. Sustain. Energy Technol. Assess. 56, 103064. <https://doi.org/10.1016/j.seta.2023.103064>.
- De Mel, I., Panagiotis, D., Dorneanu, B., Klymenko, O., Mechleri, E., Arellano-Garcia, H. Global Sensitivity Analysis for Design and Operation of Distributed Energy Systems. In: 30 European Symposium on Computer Aided Process Engineering (ESCAPE30), May 24-27, 2020, Milano, Italy. <https://doi.org/10.1016/B978-0-12-823377-1.50254-8>.
- DTU Wind Energy. Global Wind Atlas. Available: <<https://globalwindatlas.info/>>. Accessed 15 mar. 2022.
- EPE. Statistical Yearbook of electricity 2017 baseline year. Empresa de Pesquisa Energética. Brasília - DF: Ministério de Minas e Energia, 2018.
- EPE. Statistical Yearbook of electricity 2020 baseline year. Empresa de Pesquisa Energética. Brasília - DF: Ministério de Minas e Energia, 2021.
- Fose, N., Singh, A.R., Krishnamurthy, S., Ratshitanga, M., Moodley, P., 2024. Empowering distribution system operators: a review of distributed energy resource forecasting techniques. Heliyon 10 (15), e34800. <https://doi.org/10.1016/j.heliyon.2024.e34800>.
- Freitas, Bruno, de, M.R., Lavinia, Hollandia, 2015. Micro e Minigeração no Brasil: Viabilidade Econômica e Entraves do Setor (may). FGV Energia, Rio de Janeiro, pp. 1–22.
- Gabrielli, P., Gazzani, M., Martelli, E., Mazzotti, M., 2018. Optimal design of multi-energy systems with seasonal storage (jun). Appl. Energy v. 219, 408–424 (jun).
- Gamarra, C., GUERRERO, J.M., 2015. Computational optimization techniques applied to microgrids planning: a review. Renew. Sustain. Energy Rev. 48, 413–424.
- GAMS Development Corporation. General Algebraic Modeling System (GAMS) Release 36.1.0, Fairfax, VA, USA, 2021.
- Global Solar Council. Brazil accelerates in solar PV energy and becomes the eighth largest country in the world ranking of the source, informs ABSOLAR, 2024. Available at: <https://www.globalsolarcouncil.org/news/brazil-accelerates-in-solar-pv-energy-and-becomes-the-eighth-largest-country-in-the-world-ranking-of-the-source-informs-absolar/>. Last accessed on September, 23rd, 2024.
- Hawkes, A.D., LEACH, M.A., 2009. Modelling high level system design and unit commitment for a microgrid. Appl. Energy.
- Kamal, M.M., Ashraf, I., Fernandez, E., 2023. Optimal sizing of standalone rural microgrid for sustainable electrification with renewable energy resources. Sustain. Cities Soc. v. 88, 104298.
- Karamov, D.N., Sidorov, D.N., Muftahov, I.R., Zhukov, A.V., Liu, F., 2021. Optimization of isolated power systems with renewables and storage batteries based on nonlinear Volterra models for the specially protected natural area of lake Baikal. J. Phys.: Conf. Ser. v.1847 (n. 1), 012037. <https://doi.org/10.1088/1742-6596/1847/1/012037>.
- Lee, J., Guo, J., Choi, J.K., Zukerman, M., 2015. Distributed energy trading in microgrids: a game-theoretic model and its equilibrium analysis. IEEE Trans. Ind. Electron. 62 (6), 3524–3533.
- Li, Y., Han, M., Shahidehpour, M., Li, Y., Long, C., 2023b. Data-driven distributionally robust scheduling of community integrated energy systems with uncertain renewable generations considering integrated demand response. Appl. Energy 335, 120749. <https://doi.org/10.1016/j.apenergy.2023.120749>.
- Li, Y., Sun, Y., Wang, Q., Sun, K., Li, K.J., Zhang, Y., 2023. Probabilistic harmonic forecasting of the distribution system considering time-varying uncertainties of the distributed resources and electrical loads. Appl. Energy 329, 120298. <https://doi.org/10.1016/j.apenergy.2022.120298>.
- Macedo, Isaias C., 2001. Geração de energia elétrica a partir de biomassa no Brasil: situação atual, oportunidades e desenvolvimento. Cent. De. Gest. ào e Estud. Estratégicos 12.
- Mashayekh, Salman, et al., 2018. Security-constrained design of isolated multi-energy microgrids. IEEE Trans. Power Syst. 33 (3), 2452–2462.

- Mavromatis, Georgios, OREHOUNIG, Kristina, CARMELIET, Jan, 2018. Design of distributed energy systems under uncertainty: a two-stage stochastic programming approach. *Appl. Energy* v. 222, 932–950.
- Mechléri, Evgenia, Dorneanu, Bogdan, Arellano-Garcia, Harvey, 2022. A Model Predictive Control-Based Decision-Making Strategy for Residential Microgrids. In: Eng., [S.L.], v. 3. MDPI AG, pp. 100–115, should be <https://doi.org/10.3390/eng3010009>.
- Mehléri, Eugenia, Sarimveis, D., Haralambos, Markatos, Nikolaos, C., Papageorgiou, Lazaros G., 2012. A mathematical programming approach for optimal design of distributed energy systems at the neighbourhood level. *Energy* 44 (1), 96–104.
- Mustafa, George de Souza, 2010. Avaliação Econômica de Projetos Industriais. Univ. Salvador. Salvador. v. 1, 53.
- NASIR, M.N.M., MUTALE, J., 2016. Optimal sizing of solar FV/battery and biogas generator in remote microgrid. 51st International Universities Power Engineering Conference (UPEC) 1–6. <https://doi.org/10.1109/UPEC.2016.8114136>.
- NBR 13103. Norma Brasileira ABNT NBR 13103. Instalação de aparelhos a gás para uso residencial – Requisitos. Quarta edição, na, ISBN 978-85-07-04182-5.
- Neoenergia Coelba. Serviços: Residencial. 2020. Available: (<https://servicos.neoenergiacoelba.com.br/residencial-rural/Pages/Baixa%20Tens%C3%A3o/tarifa-branca.aspx>). Last accessed 5 May 2022.
- Omú, A., Choudhary, R., Boies, A., 2013. Distributed energy resource system optimisation using mixed integer linear programming. *Energy Policy* v. 61, 249–266.
- Otim, George, Okaka, D., Kayima, J., 2006. Design of a biogas plant for rural households in Uganda (Case Study: Apac District). Second Int. Conf. Adv. Eng. Technol. 544–550.
- Pallabazzer, Rodolfo, 2003. Parametric analysis of wind siting efficiency (Nov.). *J. Wind Eng. Ind. Aerodyn.* v. 91 (n. 11), 1329–1352. <https://doi.org/10.1016/j.jweia.2003.08.002>.
- Panda, A., Dauda, A.K., Chua, H., Tan, R.R., Aviso, K.B., 2023. Recent advances in the integration of renewable sources and storage facilities with hybrid power systems. *Clean. Eng. Technol.* 12, 100598. <https://doi.org/10.1016/j.clet.2023.100598>.
- Patel, P., Sivaiah, B., Patel, R., 2022. Approaches for finding optimal number of clusters using K-means and agglomerative hierarchical clustering techniques. 2022 Int. Conf. Intell. Controll. Comput. Smart Power ICICCS 1–6. <https://doi.org/10.1109/ICICCS53532.2022.9862439>.
- Ren, Fukang, Wei, Ziqing, Zhai, Xiaoqiang, 2022. A review on the integration and optimization of distributed energy systems. *Renew. Sustain. Energy Rev.* v. 162. <https://doi.org/10.1016/j.rser.2022.112440>.
- Rossum, Van G., DRAKE J.R., F.L. Python reference manual. Centrum voor Wiskunde en Informatica Amsterdam; 1995.
- Sahinidis, N.V., BARON 21.1.13: Global Optimization of Mixed-Integer Nonlinear Programs, User's manual, 2021.
- Schütz, T., Hu, X., Fuchs, M., Müller, D., 2018. Optimal design of decentralized energy conversion systems for smart microgrids using decomposition methods. *Energy* 156, 250–263. <https://doi.org/10.1016/j.energy.2018.05.050>.
- Seyedeh-Baragh, S., Abapour, M., Mohammadi-Ivatloo, B., Shafie-Khah, M., Laaksonen, H., 2024. Optimal scheduling of a microgrid based on renewable resources and demand response program using stochastic and IGDT-based approach. *J. Energy Storage* 86, 111306. <https://doi.org/10.1016/j.est.2024.111306>.
- Shi, Z., Zhang, T., Kiu, Y., Feng, Y., Wang, R., Huang, S., 2023. Optimal design and operation of islanded multi-microgrid system with distributionally robust optimization. *Electr. Power Syst. Res.* 221, 109437. <https://doi.org/10.1016/j.epsr.2023.109437>.
- Sidnell, Tim, CLARKE, Fiona, DORNEANU, Bogdan, MECHLERI, Evgenia, ARELLANO-GARCIA, Harvey, 2021a. Optimal design and operation of distributed energy resources systems for residential neighbourhoods (nov.). In: Smart Energy, [S.L.], v. 4. Elsevier BV, 100049. <https://doi.org/10.1016/j.segy.2021.100049>.
- Sidnell, Tim, Dorneanu, Bogdan, Mechleri, Evgenia, Vassiliadis, Vassilios S., Arellano-Garcia, Harvey, 2021b. Effects of Dynamic Pricing on the Design and Operation of Distributed Energy Resource Networks, 28 jul. In: Processes, [S.L.], v. 9. MDPI AG, p. 1306. <https://doi.org/10.3390/pr9081306>.
- Statista. Bioenergy capacity worldwide from 2009 to 2023. Available at: <https://www.statista.com/statistics/476338/global-capacity-of-total-bioenergy/#:~:text=Global%20capacity%20of%20bioenergy%20power%202009%2D2023&text=In%202023%2C%20the%20global%20capacity,energy%20like%20wood%20and%20manure>. Last accessed on September, 23rd, 2024.
- Tan, Wen Shan, Hassan, Mohammad Yusri, Majid, Md. Shah, Abdul Rahman, Hasimah, 2013. Optimal distributed renewable generation planning: a review of different approaches. *Renew. Sustain. Energy Rev.* 18, 626–645.
- Tawarmalani, M., Sahinidis, N.V., 2005. A polyhedral branch-and-cut approach to global optimization. *Math. Program.* v. 103 (n.2), 225–249.
- Teichgraeber, H., Lindemann, C.P., Baumgärtner, N., Kotzur, L., Stolten, D., Robinius, M., Bardow, A., Brandt, A.R., 2020. Extreme events in time series aggregation: a case study for optimal residential energy supply systems. *Appl. Energy* v. 275, 115223.
- Tooryan, F., HassanzadehFard, Collins, E.R., Jin, S., Ramezani, B., 2020. Smart integration of renewable energy resources, electrical, and thermal energy storage in microgrid applications. *Energy* v. 212, 118716.
- Wakui, Tetsuya, YOKOYAMA, Ryohei, 2014. Optimal structural design of residential cogeneration systems in consideration of their operating restrictions. *Energy* 64, 719–733.
- Weber, C., SHAH, N., 2011. Optimisation based design of a district energy system for an eco-town in the United Kingdom. *Energy* 36 (n. 2), 1292–1308.
- WEISS, W.; SPÖRK-D. Solar Heat Worldwide 2020 - Global market development and trends in 2019. Science and Technology for the Built Environment, [S. l.], v. 24, n. 8, p. 819–819, 2019.
- World Bank Group. Global Solar Atlas. Available: <https://globalsolaratlas.info/map?c=-13.859414,-42.220459,7&s=-12.972442,-38.441162&m=site&pv=small,0,12,1>. Accessed 15 mar. 2022.
- Wouters, C., Fraga, E.S., James, A.M., 2015. An energy integrated multi-microgrid, MILP (mixed-integer linear programming) approach for residential distributed energy system planning – a South Australian case-study. *Energy* v. 85, 30–44.
- Yse, Diego Lopez. The Anatomy of K-means: A complete guide to K-means clustering algorithm. Medium. 2019. Available at: <https://towardsdatascience.com/the-anatomy-of-k-means-c22340543397>. Accessed 26 jun. 2022.
- Zatti, Matteo, Gabba, Marco, Freschini, Marco, Rossi, Michele, Gambarotta, Agostino, Morini, Mirko, Marteli, Emanuele, 2019. k-MILP: a novel clustering approach to select typical and extreme days for multi-energy systems design optimization. *Energy* v. 181, 1051–1063.
- Zhang, Di, Evangelisti, Sara, Lettieri, Paola, Papageorgiou, Lazaros G., 2015. Optimal design of CHP-based microgrids: multiobjective optimisation and life cycle assessment. *Energy* 85, 181–193.